

**ANALYSIS OF DIVERSE CROSSLINKING
COMPOUNDS FOR HVDC CABLES CONCERNING
BYPRODUCTS PRODUCED IN THE MAKING**

Jessica Malmberg

Master of Science Thesis

Supervisor: Carl-Eric Wilén

Laboratory of Polymer Technology

Faculty of Science and Engineering

Åbo Akademi

February 2019

ABSTRACT

The purpose of this degree thesis is to understand the structural and production difficulties of a high voltage cable operating with direct current, and to have a look at different crosslinking compounds that are used when producing the cables with the base in existing patents from different companies. Three existing crosslinking compounds are compared with one crosslinking compound that is made at the Laboratory of Polymer Chemistry at Åbo Akademi, a new compound in the field. The thesis is done in cooperation with Maillefer Extrusion Oy.

This thesis will analyze the different crosslinkers' behaviors and resulting properties of a sample made at a pilot machine at Maillefer Extrusion Oy. The results obtained are analyzed for information that will benefit the company and make the production of cables more efficient.

The new crosslinking compound from Åbo Akademi University is an azo compound which in theory, could give better byproducts in the manufacturing process compared to peroxides that are currently used. Results show that the existing cable insulation recipes are better than the recipe with the new azo compound made at Åbo Akademi University. The degree of crosslinking gives a looser structure for the system compared with the existing insulations. Resistivity appears to be decreasing with higher voltage for the Åbo azo sample. The time it takes for the Åbo azo sample to crosslink is also longer than the others and need slightly higher temperatures, which is also a problem. It should be kept in mind that the manufacturing process with Åbo azo is not yet optimized. The results obtained from tests are promising for the compound but should be further investigated.

Keywords: HVDC cable, peroxide, azo compounds, crosslinking

REFERAT

Avsikten med arbetet var att förstå strukturen för högspänningskablar och problemställningar för produktionen av en kabel med likström. Därtill även förstå och applicera olika tvärbindingämnen som resulterar i ett tvärbundet system i LDPE som används för insolationen för en högspänningskabel. På basen av tre patenter angående insolation för en högspänningskabel med likström, görs prover som jämförs med ett nytt recept med ett nytt tvärbindingämne som framställts på Åbo Akademi. Alla prover innehåller olika tvärbindingämnen och de jämförs med varandra angående tvärbindningsstruktur, tid det tar för att uppnå ett tvärbundet system, ledningsförmåga och mekaniska egenskaper. Det här projektet är ett samarbete med Maillefer Extrusion Oy, var även en pilotmaskin fanns till förfogande under arbetet för kabelprover.

Målet med undersökningen är att kunna utveckla kablar som kan transportera ström från källan till kunden på en längre sträcka än vad man kan för tillfället.

Resultaten i undersökningen visar att det existerande varianterna av insolationer har bättre egenskaper än vad den nya föreningen har. Tvärbindningsgraden är klart sämre än vad de befintliga recepten ger; en lösare struktur fås då det nya tvärbindingämnet används. Ledningsförmågan sämre hos insolationen med det nya ämnet. Tiden det tar för nya ämnet att tvärbindas är även längre och kräver en aningen högre temperatur än vad befintliga. Till slut bör påpekas att det nya ämnet är en azoförening, vilket betyder möjligen bättre bi-produkter som uppstår jämfört med befintliga peroxid-baserade system. Man bör även tänka på att justera mängden tvärbindare, vilket leder till möjliga följd undersökningar. Tvärbindaren ser lovande ut och är i rätt riktning men behöver optimeras och undersökas mer för att bekräfta om produkten kan bli bättre.

Sökord: HVDC kabel, högspänd likströmskabel, peroxid, azoförening, tvärbinding

Jessica Malmberg

ACKNOWLEDGMENTS

I would like to thank Carl-Eric Wilén for introducing me to the matter and the company, moreover helping me by guiding throughout the thesis. I also would like to thank all who helped me with the instruments in the polymer technology laboratory and analyzing results from the tests. Moreover, I would like to thank every other person that did some more advanced analysis that I was not capable to do by myself, persons who synthesized the azo-compound and Maillefer for taking time to extrude samples at the pilot machine.

Helsinki, February 2019

Jessica Malmberg

CONTENTS

ABSTRACT	2
REFERAT	3
ACKNOWLEDGMENTS	4
AIM	12
1 INTRODUCTION	13
1.1 Structure and development of a high voltage cable	13
1.2 AC and DC current cables	15
1.3 Insulation and remaining challenges	17
1.3.1 <i>Requirements for the insulation</i>	18
2 INSULATION	19
2.1 Polyethylene	19
2.2 Extrusion	20
2.3 Crosslinking	21
2.3.1 <i>Decomposition of peroxides</i>	24
2.4 Patents review	25
3 METHODS	27
3.1 Sample preparation for specimen in lab	27
3.2 Pilot machine samples.....	28
3.3 Byproducts - Pyro-GC/MS	29
3.4 Thermogravimetric analysis - TGA.....	31
3.5 Structure analysis - FTIR.....	31
3.6 Differential scanning calorimeter – DSC	31
3.7 Crosslinking rate - Rheology	32
3.8 Degree of crosslinking - NMR.....	37
3.9 Conductivity	38
3.10 Gel content	38
3.11 Mechanical properties	39
4 RESULTS	40
4.1 Pyro-GC/MS	40
4.2 Rheology.....	43
4.3 DSC	47
4.4 FTIR.....	49
4.5 NMR.....	52
4.6 Gel content	53

4.7	Tensile test	53
4.8	Conductivity	55
5	CONCLUSIONS AND SUMMARY	57
	REFERENCES	61
	SWEDISH SUMMARY	65
	APPENDICES	71
	Appendix A – Recipes	71
	Appendix B – Process parameter data from pilot machine	73

Figures

Figure 1. High voltage cable structure. [4]	13
Figure 2. Polymer chain arrangement of semi-crystalline polymer and spherulite formation. [11]	17
Figure 3. Dicumyl peroxide molecule forming radicals.	20
Figure 4. Left Triallyl Cyanurate (TAC) molecule and right Triallyl Isoyanurate (TAIC).	20
Figure 5. TAIC molecule crosslinking mechanism. [14]	21
Figure 6. Co-agents initiated crosslinks indicated by arrows and direct carbon-carbon crosslinks by circle. [12]	22
Figure 7. The structure of an azo compound.	22
Figure 8. Decomposition of dicumyl peroxide and formation of by-products. [12]	23
Figure 9. Decomposition and radical formation of Trigonox 101. [17]	24
Figure 10. Schematic view over how recipes are used from the different patents in different samples.....	27
Figure 11. To the left azo compound used for sample 3 - Cyclohexyl(tert-octyl)diazene and to the right di-tert-butyl azodicarboxylate (DBAC).	28
Figure 12. Synthetication of cyclohexyl(tert-octyl)diazene aka Åbo Akademi azo compound. [19]	28
Figure 13. Rheology measurements are based on shear forces applied on a matter.	34
Figure 14. Example of a frequency sweep oscillatory measurement - Storage (G') and loss modulus (G''). [23]	34
Figure 15. Oscillation measurement showing the correlation between measured strain phase shift and phase angle. [24]	35
Figure 16. Plate - plate shearing rheometer. Arrow is showing the oscillation motion. [25]	35
Figure 17. Rheology measurement scheme of the curing time.	36
Figure 18. Tan delta with time showing the absolute curing time for a typical thermosetting polymer. [23]	37
Figure 19. Decomposition products of Åbo azo compound.	42
Figure 20. Time sweep of sample 1.1 - How t_{90} is determined.	43
Figure 21. Temperature ramp rheological measurement to determine optimum curing temperature range.	44
Figure 22. DSC Heating curve of samples from the pilot machine	46

Figure 23. DSC cooling curve of samples from the pilot machine	47
Figure 24. Ineos BDP - 2000 FTIR	48
Figure 25. FTIR spectra of all non-crosslinked samples.	49
Figure 26. Triallyl isocyanurate (TAC) FTIR spectra. [28]	49
Figure 27. FTIR of samples from the pilot machine.	50
Figure 28. ¹ H NMR solid echo experiment run on the different samples made at the pilot machine.	51
Figure 29. Tensile test data of all samples in a stress - strain diagram	54
Figure 30. Resistivity measurements of Borealis DC, SILEC and Åbo azo samples exposed to three different electrical fields.	55

Tables

Table 1. List of possible by-products in the different samples.	30
Table 2. Substances found in py-GC-MS test	40
Table 3. Data of the curing time based on rheological dynamic time sweep for different temperatures.....	45
Table 4. DSC data obtained from graphs	47
Table 5. Soxhlet extraction results giving the gel content of the different crosslinked samples from Maillefer.	52
Table 6 Mechanical properties of all samples in room temperature	53
Table 7. Mechanical properties of all samples in 95°C	53
Table 8. Resistivity results measured in 60°C	55

ABBREVIATIONS

AC	Alternating current
DC	Direct current
HV	High voltage
MP	Mass impregnated
HVDC	High voltage direct current
XLPE	Crosslinked polyethylene
PP	Polypropylene
LDPE	Low-density polyethylene
PE	Polyethylene
VSC	Voltage-source converter
DCP	Dicumyl peroxide
CSC	Current Source Converter
TAC	Triallyl cyanurate
TAIC	Triallyl isocyanurate, also TAICROS
DBAC	Di-tert-butyl azodicarboxylate
GC/MS	Gas-chromatography mass-spectrometry
TGA	Thermogravimetric analysis
FTIR	Fourier Transform Infrared Ray
DSC	Differential scanning calorimeter
T_m	Temperature at melt
T_c	Temperature of crystallization
T_g	Glass transition temperature
H_m	Enthalpy of melting peak
H_0	Heat of fusion of 100% crystalline polymer
τ	Shear stress
γ	Shear strain
$\dot{\gamma}$	Shear rate
G'	Storage modulus
G''	Loss modulus
δ	Phase angle
η	Viscosity
M	Torque

Jessica Malmberg

DMA Dynamic Mechanical Analysis

NMR Nuclear magnetic resonance

C Carbon

AIM

The aim of this master's thesis was to explore different ways to prepare enhanced crosslinked low-density polyethylene (LDPE) insulating material for high voltage direct current cables (DC cables). The main targets were to produce an insulating material with improved dielectric properties, meaning low electrical losses even over long distances of > 500 km. Furthermore, an insulating material free of polar byproducts, such as cumyl alcohol and acetophenone or any compound that is polar. Lastly, also improve the degree of crosslinked material. All this to prevent breakdown even at elevated temperatures. The recipes used in this thesis were based on patents by Borealis, ABB and SILEC Cable. The insulating materials were prepared utilizing radical generators based on peroxides and azo initiators with or without additional crosslinking agents. Especially the azoalkane crosslinking was deemed to be of great interest. The ABB patent uses an azo compound for crosslinking and an azo compound is also developed at Åbo Akademi University for crosslinking of polyolefins.

In general, the foreseeable benefits of using azo initiators over peroxides for crosslinking of DC cables are:

- Unlike peroxides, azo compounds do not produce polar byproducts that would impair electrical insulation properties.
- No degassing required due to no polar byproducts that would potentially cause local electrical field enhancements and finally breakdown.
- The higher decomposition of azo compounds in comparison to peroxides allows homogenous blending of azo compounds in polyolefin prior to actual crosslinking, thereby avoiding discontinuities in the crosslinked material. Furthermore, one would avoid uncontrolled exothermic reactions, known as scorch, and allow homogeneous distribution of crosslinks.

1 INTRODUCTION

1.1 Structure and development of a high voltage cable

The first cables designed for high voltage (HV) use, were insulated with oil-impregnated paper, so called mass impregnation (MP). The insulation was further developed and replaced with oil-filled MP cables, where the oil was pressurized and of low viscosity. In 1999, the modern HV cable operating with DC became available with crosslinked polyethylene insulation. A lot of improvements have been made since then. Different types of cable lay-ups and modifications to the polymer using different additives, have led more profitable ways of transmitting high voltage safely, as well as enabling transmission at higher voltage. [1]

A typical high voltage direct current (HVDC) cable today consists of a single conductor rod in the middle, usually made of copper or aluminum. The rod transmits the power from A to B with as little resistance as possible. The next layer is the inner semi-conductive layer, which is usually made of the same base polymer as the main insulation material itself. It is a thin layer and its purpose is to seamlessly bring and adhere the conductor and the main insulation together. The second layer exists on the other side of the insulation as well, called outer semi conductive layer. The conductive properties of these layers create a radial field, which prevents the transfer of leaking charges into the insulation. Inorganic fillers that are added to the polymer provide the semi-conductive properties. [1]

The insulation material is made of crosslinked polyethylene, XLPE, with the purpose to resist the voltage transmitted. The insulation is extruded with or without the two semi-conductive layers directly onto the conductor rod; the whole package is then crosslinked together for maximum strength and durability. Other plastics, such as polypropylene, PP, have also been tested due to its higher melting point and due to the fact that XLPE is not recyclable. The focus stays on LDPE in this study and it was used as the base polymer. [1]

The semi-conductive layers have a conductivity that is remarkably higher than the insulating layer. The semi-conductive layer contains inorganic fillers such as carbon black, metal oxides and carbonates to increase volumetric resistivity. Volumetric resistivity for LDPE lies around 1600-1800 $\Omega\cdot\text{m}$, but adding fillers can reduce resistivity to 100-1000 $\Omega\cdot\text{m}$, which leads to increased conductivity in the first layer. [2] The insulating layer should preferably be thick in comparison to the semi-conductive layer to keep low conductivity through the whole insulating system. The thickness of the semi-conductive layer corresponds to the breakdown probability, which is reduced with increasing thickness of the inner semi-conductive layer. [3]

Furthermore, the cable has a metallic screen layer or a sheet that adds strength and a radial field to the cable. The metal screen is always grounded for safety. The low-resistant metal provides an easy way for a short-cut current to travel, if such an incident occurs. The metallic screen can be a full sheet of metal, which then also works as a humidity barrier. In other cases, water blocking or a sealing system is added onto the metallic sheet in the form of hydroscopic powders or tapes, which prevent moisture or water from spreading in longitudinal directions, if the cable is punctured. [1]

The outermost layer of a typical land cable is a thermoplastic cover to protect against moisture and external factors, such as galvanic or electrolytic actions, as well as adding extra protection when the cable is mounted. If the cable is designed for underwater applications, a metallic armor is applied for proper protection and covered up with PE yarn to add roughness to the surface. Figure 1 shows the structure of the cable. [1]

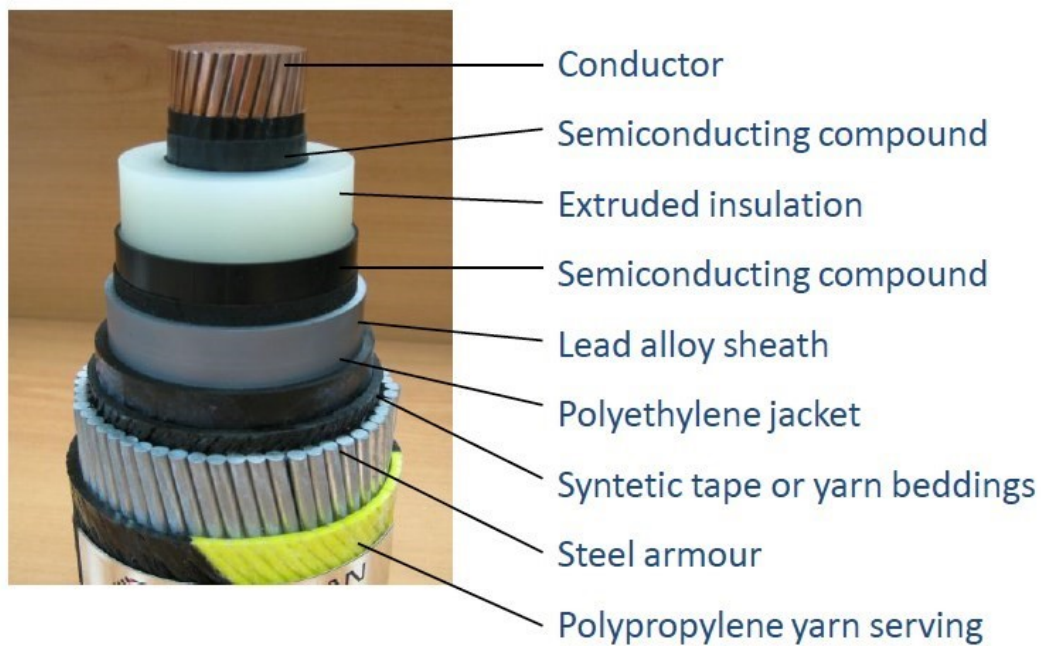


Figure 1. High voltage cable structure. [4]

1.2 AC and DC current cables

The alternating current (AC) incorporates numerous beneficial features concerning power transmission. The first distribution systems were of an AC-type because of the stability, easy maintainance and for economic reasons. However, the properties were less suited for long transmission ranges than DC-types. This has led to an increase of DC-lines over the last 10 years. AC-lines are, however, still the dominant type when it comes to underground cables. Listing the advantages and disadvantages in AC and DC systems explains why DC cables are today the research subject and also the background for this master's thesis. [5]

First of all, cables behave like large capacitors and they 'load up' when voltage is applied. When the cable is 'fully loaded', power is coming through the other end. With AC systems the current is constantly changing directions, meaning it will charge up every half cycle. Here lies the problem with AC systems, since they do not manage distances very well, a lot will go wasted in relation to what comes out from the other end. DC systems will not have this transmission problem, because once the cable is charged, it stays charged. [5]

The local magnetic field created by an AC current will cause problems with nearby cables and lead to a current crowding effect. The crowding is enhanced with increased frequency and will affect the system by an increase in resistance. [1]

AC cables have problems with transmission due to the inductive and capacitive properties of an AC system, which affects the capacity and the transmission distance. Direct connection of two AC cables is not possible, if the two cables are operating with different frequencies. AC lines will need terminals along the way. [1]

A terminal for DC transmitters is more expensive than an AC terminal, but a DC line will only need one terminal at each end, which is an AC to DC converter at one end and a DC to AC converter at the other. Therefore, the cost of AC lines will drastically increase with distance compared to DC lines. Hence, there will be a point where DC lines become more feasible than AC lines from an economical point of view, when the terminal and cable costs are considered. Generally, if the transmission distance is over 50 km the DC line will be more feasible. [6]

Because DC transmissions do not need mid-way terminals, they can be applied in undersea applications for bulk power transmission from power harvesting stations offshore. Additionally, DC lines do not introduce crowding in the same manner as AC lines do. Electric losses are minimal and usually neglected, unlike in AC systems. The average field stress of a DC line is in general higher than an AC line, which means that the line can transport more power at higher voltage per unit length. Typical mean field stress values for DC lines are 11-18 kV/mm and for AC lines 7-16 kV/mm. [1]

Disadvantages with DC lines are the costs and losses an AC to DC converter terminal causes. Such a terminal is called a current source converter (CSC), and it has its limitations and technology issues. Half of the transmitted active power goes to the power demand for the AC nodes at the site. The losses can be reduced if the converters have on-load tap changers to control the AC voltage. Other components needed at the stations are for instance power harmonics, filters and capacitor banks. There is no need to go into

further detail about the electric systems at the stations or terminals within the scope of this thesis. [1]

1.3 Insulation and remaining challenges

The insulation of HVDC cables has been a highly researched topic for a long time now. It is also the topic of investigation in this thesis. Matters of interest are the crosslinking process, byproducts formed during the manufacturing process and general structural analysis of the insulating material.

The insulation in high voltage cables are made of crosslinked low-density polyethylene (XLPE). Crosslinking agents introduced to the polymer matrix are added in small amounts, a maximum of 2 wt%. Peroxides are the most widely used compounds, for example dicumyl peroxide (DCP). DCP decompose to a wide range of volatile compounds such as methane, acetophenone and cumyl alcohol, which are the typical compounds formed during the decomposition of peroxides in general. The formed byproducts are problematic when they are left within the material matrix, since among other things they accumulate space charges. The polarity of the molecule and the state of the substance (gaseous or nongaseous) determine how much the electrical properties are affected. A degassing method can be used to minimize the concentration of formed byproducts; the process is time consuming and therefore not desired. [6]

When replacing AC with DC lines at the beginning of the 21th century the old insulation type became a problem for DC systems. Direct current creates space charges in the polymer matrix that result in non-uniformed distribution of the stresses in the material. Due to polymers' resistivity, the space charges tend to last for a long time in the matrix creating polarized patterns which act like capacitors. The problem arises when reversing the current and changing the polarity. The reversing can lead to an electrical breakdown. Hence, voltage-source converters are used to prevent the breakdown when the current is reversed. The following chapter will discuss more thoroughly the complications and challenges of the insulation for a DC system. [7]

1.3.1 Requirements for the insulation

Critical parameter for high voltage cable insulations is heat resistance, which prevents decomposition and degradation during operation. The temperatures reach 100 °C in use. Mechanical strength is also needed to prevent deformation, abrasion and creep. The insulation needs to tolerate electrical stresses, especially in DC systems where the polarity of the current can be changed. A stable insulation resistivity is anticipated and it should not be affected by the surrounding conditions, such as temperatures and electrical stresses. [8]

Thermal properties of the cable should be taken into consideration, how the insulation is affected by the electric field changes. Heat is generated inside the cable via a leaking current that stays trapped in the insulation in between the inner and outer semi-conductive layer. The generated heat must be able to leave the matrix, hence the thickness of the insulating layer is restricted. The leakage depends on the insulation, its capability to handle the electric field as well as the DC conductivity. DC conductivity of the material can result in thermal runaway under excessive heat formation and stresses. Depending on the electric field applied, an increase in the field will generate more heat. Therefore, DC conductivity must stay as low as possible in the insulation material. [9]

The insulation should also have low space charge retaining properties. Space charges are built up by charges being trapped in uneven morphologies of the insulating layer, such as clusters of additives, dirt, dust, defects and compounds (byproducts) that were formed during the extrusion and crosslinking process. Space charges cause uneven electric fields and can result in accelerated ageing and electrical breakdown when the polarity of the voltage is changed. Hence, the insulating material should be clean and free from byproducts. Should an electrical breakdown occur, the insulation should have the ability to protect and interrupt the breakdown to prevent a continuous arc. An electrical breakdown occurs when the voltage applied exceeds the breakdown voltage of the material, which means the insulator should have a high breakdown strength. [1]

2 INSULATION

2.1 Polyethylene

Polyethylene is a versatile multipurpose polymer; it can be adapted to a very wide range of applications by using different polymerization and production methods. In HVDC cables, low-density polyethylene (LDPE) is used and is therefore the focus of this thesis. LDPE is semi-crystalline by its nature, has a melting point of about 115 °C and crystallinity that varies from 45 to 55%, which depends on the cooling rates, processing methods and the polymer grade. [10]

The LDPE has crystalline and amorphous regions in its polymer matrix, hence semi-crystalline. The lamellae are connected via tie chains, which contributes to the strength and ductility, whereas the crystalline regions contribute with the rigidity and high softening temperatures. The lamellae form three-dimensional spherulite structures, which form the polymer's 'crystals'. Figure 2 is a schematic illustration of a spherulite and how it is formed, the crystalline and amorphous regions can also be seen.

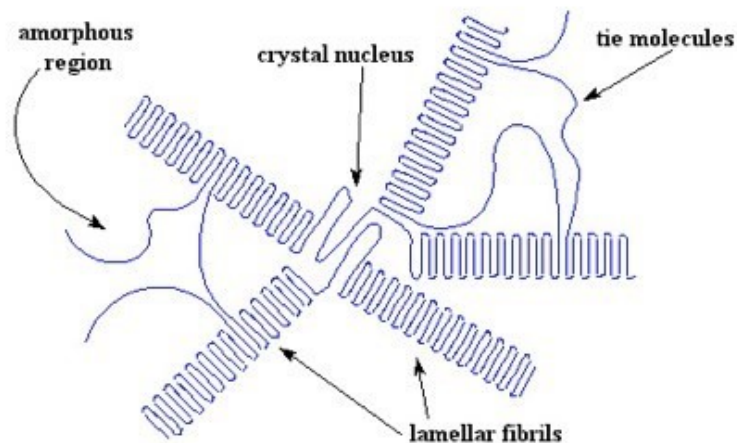


Figure 2. Polymer chain arrangement of semi-crystalline polymer and spherulite formation. [11]

Crosslinking LDPE improves properties that are beneficial for the cable insulation. Crosslinking is accomplished by initiating links in between chains to form a stiffer

structure. Crosslinking can be achieved by free radical reactions, with for example peroxides, and further enhanced via tetra-active molecules containing for instance vinyl groups. [12] Crosslinking the polymer gives a higher load-bearing capacity, creep resistance, stress relaxation, tear resistance and compression strength. Other positive changes for HV cable applications are lower heat capacity and thermal expansion, increasing heat distortion temperature, tensile strength and reflective index. The crosslinking will also reduce the degree of crystallinity due to the restricted mobility of the chains to form lamellae, which results in a lower modulus. [13]

2.2 Extrusion process

The extrusion process of a high voltage cable is described in a paper by Smedberg et al. [9] as, starting from the inner out: inner semi-conductive layer, insulation layer and outer semi-conductive layer, all of which are extruded in layers directly onto the metallic conductor rod seamlessly. The crosslinking happens directly after the extrusion in a vulcanization pipe maintaining right pressure, temperature and duration.

The crosslinking process is initiated by activation of the radical generators by heating or by irradiation. The initiators are substrates that form free radicals in the system, which introduce bonds between the polymer backbones. The crosslinked system make a material with improved mechanical and physical properties. The crosslinking procedure is forming byproducts at this stage. One way of eliminating the harmful byproducts is by degassing. The degassing process is, however, both energy and time consuming and hence not economical for the production. [9]

The crosslinking agents are recommended not to exceed 2 wt% of the total amount of polymer. The amount depends on the number of functional groups in the crosslinking agents, which means that the ratio of added agents depends on which crosslinker is used with what polymer. The curing lasts for minutes up to hours at elevated temperatures. [9]

Semi-conductive layers may contain inorganic fillers to improve conductivity and prevent electrical charges from leaking into the insulation, whereas the insulation contains crosslinking agents, antioxidants and other possible additives for fulfilling the demands

on a high voltage cable. The additives are either mixed together in advance, or added under the process fed directly into the screw.

2.3 Crosslinking

Crosslinking improves mechanical and electrical properties of the cable. With increased crosslink density, the modulus, hardness, resilience and abrasion resistance of the polymer increase as well. The maximum elongation, heat build-up and stress relaxation decrease with increased crosslink density. [14] Polyethylene has a melting point of 100 °C – 130 °C, whereas crosslinked polyethylene does not melt. Electrical properties increase with crosslinking; dielectrical losses are reduced and a high electrical breakdown strength is achieved. Crosslinked PE also shows better creep properties and greater resistance to water treeing, which is the penetration of water into the plastic. This is associated with electrical treeing that eventually initiates an electrical breakdown. [12]

in 1955 Precopio and Gilbert discovered that dicumyl peroxide (DCP) works well with polyethylene, and it has been used as the standard peroxide ever since. Peroxides have a weak oxygen bond [–O–O–], that breaks at relatively low temperatures. When the temperature is rising, the bond between the oxygen atoms breaks and they form radicals. They interact with the polymer chains by abstracting a hydrogen atom, leaving a radical position to react to another radical, forming a direct link –C–C– bond. The high decomposition temperature of DCP allows its use in an extruder at relatively high processing temperatures when melting the polyethylene without significant degree of undesired pre-curing. The reaction continues until all peroxide has been consumed. The radical formation of DCP is shown in Figure 3. [13]

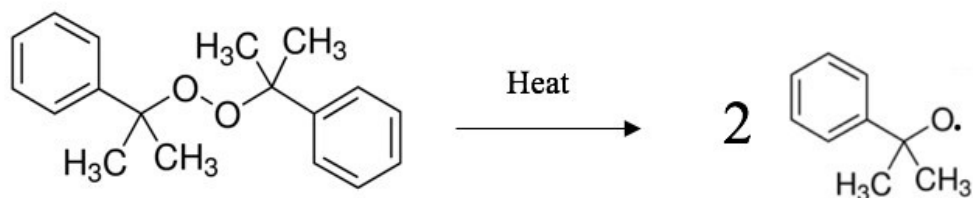


Figure 3. Dicumyl peroxide molecule forming radicals.

Crosslinks are established either by direct chain to chain, that is initiated by peroxide, forming carbon to carbon bonds $[-C-C-]$. Moreover, it can be enriched by bridging through polyfunctional coagents, such as triallyl cyanurate (TAC). TAC is a tetra-active molecule that can crosslink in several directions due to the three vinyl groups, see Figure 4. [15] Another tetra-active molecule that will be used in this thesis is TAIC, triallyl isocyanurate, which in fact is a claisen rearrangement of TAC.

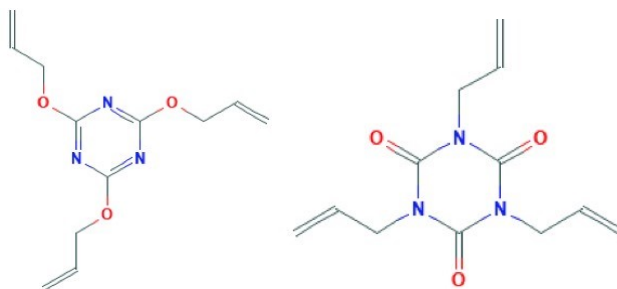


Figure 4. To the left triallyl cyanurate (TAC) molecule and to the right triallyl isocyanurate (TAIC).

A. Smedberg et al. have shown that vinyl groups are rapidly reacting first along with the peroxides giving a higher gel content due to the vinyl groups. The crosslinking reaction with TAC or TAIC is illustrated in Figure 5. The crosslinking co-agent reacts to a radical position on the polymer chain that has been formed by the peroxide. A vinyl group will react to these positions to form a carbon to carbon bond. The active radical can attach to the vinyl group and form a crosslink, but still remain reactive to react to another spot via other vinyl groups in the molecule. The resulting network is loose; however, in combination with direct radical crosslinks formed from the peroxide it results in an even stronger and tighter network. The network is illustrated in Figure 6. [16]

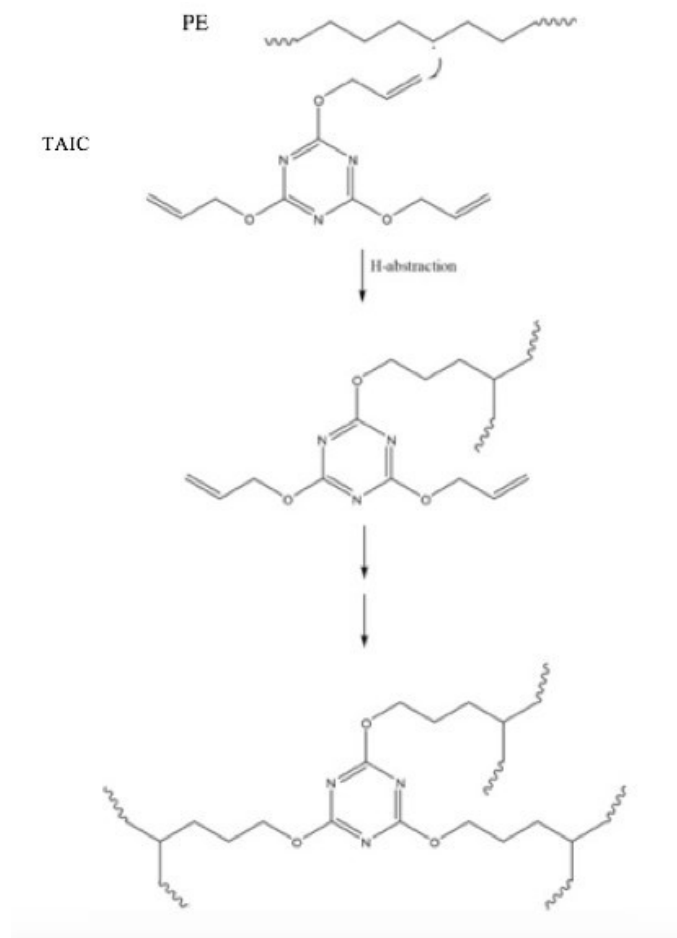


Figure 5. TAIC molecule crosslinking mechanism. [14]

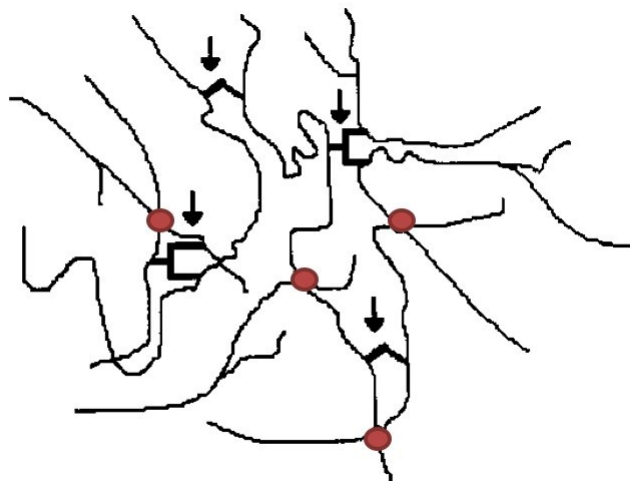


Figure 6. Co-agents initiated crosslinks indicated by arrows and direct carbon-carbon crosslinks by circle. [12]

Another crosslinking aid is azo compounds. According to a study made by Ho et al., no polar byproducts are formed by azo compounds and therefore no degassing is needed[10]. Byproducts that are formed are non-polar. The structure of an azo compound is seen in

Figure 7, where the nitrogen atoms form the signature of an azo compound. X in the figure can be a bond or an oxy-carbonyl group which, in that case, forms carbon dioxide when decomposing or remains as an oxy-carbonyl radical. R are non-polar low molecular weight functional groups such as alkyl or an aryl type of hydrocarbons. The left-over non-polar hydrocarbons are less harmful than products from DCP [10]

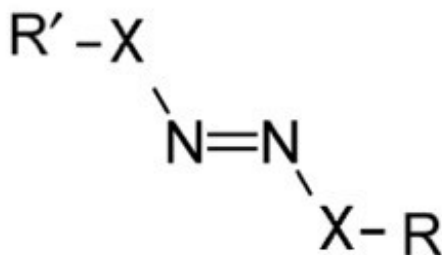


Figure 7. The structure of an azo compound.

2.3.1 Decomposition of peroxides

The decomposition of dicumyl peroxide (DCP) has been thoroughly studied over the years and the byproducts have been identified. The decomposition of DCP creates three main components, 1) methane, 2) cumyl alcohol and 3) acetophenone. The formation of these three compounds during decomposition is illustrated in Figure 8.

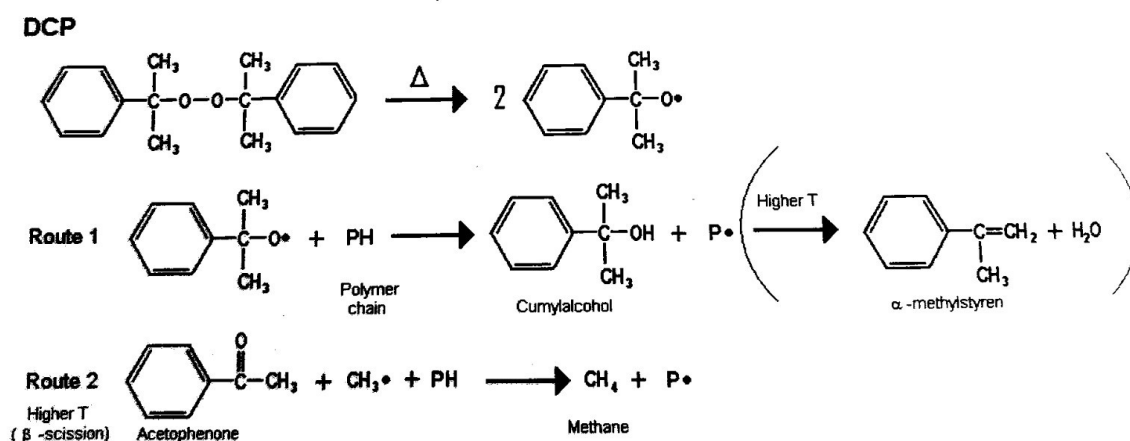


Figure 8. Decomposition of dicumyl peroxide and formation of byproducts. [12]

The products of decomposing peroxide are of interest due to interfering with the insulation properties. Byproducts formed from DCP are polar, which leads to local differences in the material and causes a non-steady system. Space charges are accumulating due to the differences in polarity of the matrix. [10]

The decomposition of another widely used peroxide, Trigonox 101, is shown in Figure 9. The formed oxygen radicals have a strong tendency to abstract hydrogen from the polyethylene backbone, where byproducts such as methane, ethane, acetone, tert-butanol and tert-amylalcohol are formed. [17]

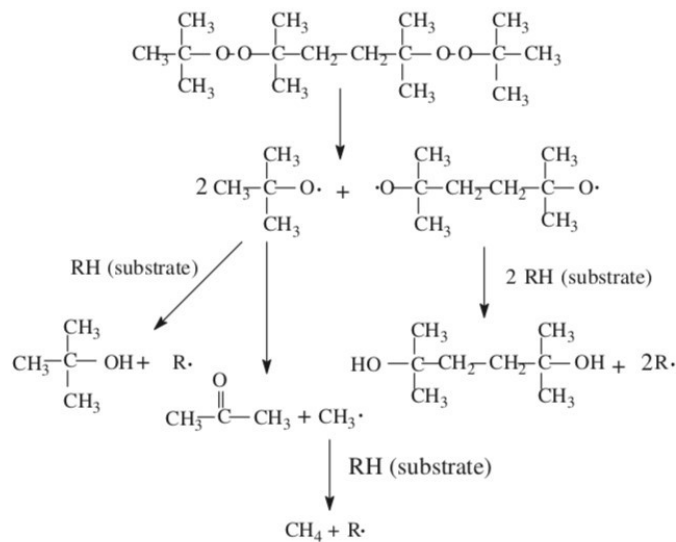


Figure 9. Decomposition and radical formation of Trigonox 101. [17]

2.4 Patents review

A brief review of the patents that have been utilized in this thesis work is provided in this chapter.

A patent from Borealis [8] has been used as a reference recipe that utilizes DCP as radical generator together with an LDPE grade that contains vinylic groups that easily undergo crosslinking to make crosslinked LDPE insulating material. The reference material is called sample 0 in the experimental part. The samples have been prepared under similar experimental conditions as in the patent, using different radical generators.

The crosslinking is initiated by increasing the temperature above 150°C. The patent [8] claims that it is only necessary to keep the reaction at elevated temperatures for 8 minutes, whereby only the surface of LDPE is crosslinked, the surface meaning the outer semi-conductive layer and a part of the insulation layer. This improve ability of connecting cables, when a part is non-crosslinked. Also, the degassing step can be reduced, since byproducts will only be present at the surface of the insulation.

In contrast to the reference patent recipe, the SILEC patent [18] utilizes the peroxide ‘Trigonox 101’ as radical generator. The co-agent used is a polyfunctional organic compound such as TAC or TAIC, preferably the TAIC derivative. The SILEC patent claims that by injecting the peroxide and co-agent in liquid form, the formation of byproducts can be limited. By using unsaturated co-agents the amount of peroxide can be reduced. The co-agents will react and form bridges with the help of peroxide and to form a large crosslinked network. This, in turn, results in less polar byproducts. Less polar byproducts mean shorter degassing time. In some cases, degassing can be avoided.

Finally, the third patent from ABB [10] is based on crosslinking with azo compounds, specifically di-tert-butyl azodicarboxylate (DBAC). The azo compound needs a co-agent for crosslinking and triallyl cyanurate (TAC) is used. DBAC has an oxy-carbonyl group which is attached between a nitrogen atom and a hydrocarbon. The oxy-carbonyl reacts and releases the two other hydrocarbons attached to the carbonyl and N₂ gas.

The crosslinking is initiated by raising the temperature, which causes the azo compound to break up and form radicals. The radicals will abstract a hydrogen from the polyolefin and leave a spot for a carbon to carbon bond to be formed in-between chains. This means the byproducts in the polymer matrix consist of small molecules or hydrocarbons that will evaporate or remain in the matrix, however not affecting the electrical properties. The patent claims that hydrocarbons do not disturb the stability of the system nor will they generate charges due to similar structure as the base polymer. No further degassing will therefore be needed.

3 METHODS

The main factors investigated in this thesis are the degree of crosslinking, curing time and decomposition products formed during the production of HVDC cables when using different types of crosslinkers and co-agents. A commercial Borealis LDPE grade for DC cables is referred to as sample 0 and it is used as the reference. Sample 0 uses dicumyl peroxide as initiator. An insulation sample using different initiators will be made in laboratory scale. Recipe 1. containing initiator Trigonox 101, 2. containing azo initiator DBAC and 3. containing an azo initiator made at Åbo Akademi University referred to as Åbo azo. The recipe described in the Borealis patent is used for all different samples 1.1, 2.1, and 3.1, whereby a comparison of the different radical generators with same ratio can be made. Sample 1.2 utilizes the SILEC [18] base recipe and 2.2 the ABB recipe [10]. In sample 3.2 an azoalkane compound, cyclohexyl(tert-octyl)diazene, Åbo azo, is used in order to compare the efficiency of the two azo compounds. A schematic overview of the samples is shown below.

	DCP	Trigonox	DBAC	Åbo azo
Borealis patent recipe	0	1.1	2.1	3.1
Silec patent recipe		1.2		
ABB patent recipe			2.2	3.2

Figure 10. Schematic overview how recipes are used from the different patents in different samples.

3.1 Sample preparation for specimen in lab

The lab mixer HAAKE rheocord system 40 with twin counter-rotating screw was used for the mixing of additives and crosslinking agents together with the polymer. LDPE pellets, grade INEOS BPD-2000, is melted at 130°C for 2 minutes at 30 rpm. Antioxidants are added into the molten polymer and mixed for a minute, thereafter crosslinking agents are added and mixed for 2 more minutes at 60 rpm.

Practical sources of error are quite evident at this stage. A maximum of 40 g can be mixed in the mixing unit and as a result the additives are measured in milligrams, which makes it difficult to get all additives into the mixing unit. A substantial amount of liquid additives ended up being stuck at the walls of the vessel poured from, and additives of fine powder were flying around when added into the mixing chamber. Hence, the actual amount of additives is almost certainly not the same as measured, though it was conducted with precision and care. The recipes, as well as the measured amounts of additives are presented in Appendix A – Recipes.

The azo compound, cyclohexyl(*tert*-octyl)diazene, synthesized at Åbo Akademi University was used for sample 3 together with a co-agent TAC. This is the same co-agent that was used in sample 2 for comparison of the two different azo compounds. The Åbo azo molecule is illustrated in Figure 11. In Figure 12, the synthesis route is shown. The major difference between DBAC azo compound and Åbo azo, is the lack of oxygen atoms. The molecule for DBAC can also be seen in Figure 11.

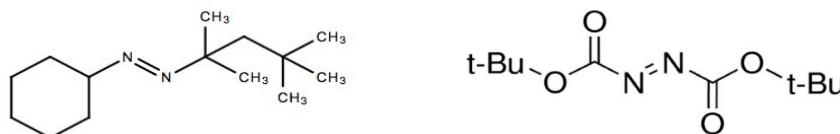
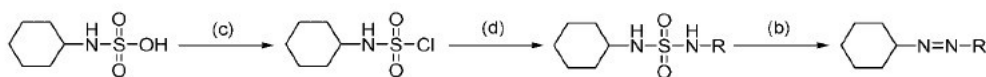


Figure 11. To the left azo compound used for sample 3 - Cyclohexyl(*tert*-octyl)diazene and to the right di-*tert*-butyl azodicarboxylate (DBAC).



(a) $\text{SO}_2\text{Cl}_2, \text{Et}_3\text{N}, \text{CH}_2\text{Cl}_2, 0^\circ\text{C}, 4\text{h}$; (b) $\text{NaOCl}, \text{NaOH}, 60^\circ\text{C}, 3\text{h}$; (c) $\text{PCl}_3, \text{toluene}, 100^\circ\text{C}, 1\text{h}$; (d) $\text{R-NH}_2, \text{Et}_3\text{N}, 0^\circ\text{C}, 5\text{h}$

Figure 12. Synthesis of cyclohexyl(*tert*-octyl)diazene aka Åbo Akademi azo-compound. [19]

3.2 Pilot machine samples

A pilot machine at Maillefer Extrusion Oy was used to make genuine cable samples. The non-crosslinked laboratory samples were used for determining specifications for the pilot machine when making the cable samples. For instance, the rheology measurements gave information about how the crosslinking was proceeding in relation to the curing time. This information was crucial for the pilot machine operation.

Sample 3 contains the new Åbo azo compound. The recipe 3.1 was used in the pilot machine, containing 1.35 wt% Åbo azo compound and co-crosslinker TAC. The pilot machine was restricted to minimum of 100 kg sample and the recipe was adjusted accordingly. In addition, there was only a limited supply of the synthesized Åbo azo compound, which meant it was just enough for one test run.

The extrusion began by cleaning the screw from residues of previous runs, directing center rods and checking the flow. Once everything was set, the azo and TAC mixture (50/50) was injected to the screw with 0.1% antioxidants. The extrusion was fed into the reaction chamber when the crosslinking compounds had been evenly distributed in the polymer matrix.

The crosslinking occurred in a closed reaction tube with a nitrogen atmosphere of 10 bar. The crosslinking took place with a programmed decreasing temperature ramp from 380 °C to 320 °C over 60 minutes, followed by 60 minutes of cooling. The process parameters used can be reviewed in Appendix B – Process parameter data from pilot machine.

3.3 Byproducts - Pyro-GC/MS

In the Pyrolysis GC/MS, the samples are pyrolyzed rapidly at 1000 °C, volatiles travel to the GC-MS where samples are analyzed.

In Table 1 is listed products that are theoretically possible to form, when pyrolyzing the pure crosslinking compounds in an oxygen atmosphere.

Table 1. List of possible byproducts in the different samples.

Recipe	Crosslinking compound	Possible byproducts
0. Borealis	DCP	Methane Acetophenone 2-phenylisopropanol Cumyl alcohol

1. Silec	TAICROS	allyl alcohol isocyanuric acid
	Trigonox 101	Acetone Tert-butanol Methane Tert-amyl-alcohol Ethane Carbon oxides
2. ABB	DBAC	Nitrogen Methane Carbon monoxide Ketones Alkyl-acetates
	TAC	No information
3. Åbo Azo	Azo compound	Hydrocarbons
	TAC	No information
Other substances that may be found		Cumyl alcohol Alfa-metyl-styrene Alfa-cumyl-alcohol Dicumyl peroxide Tert-butyl-alcohol Hydrocarbons 2-phenyl-propanol

Sources of error for the pyrolysis GC/MS are that the instrument does not detect small molecules, under 7C chains, which leaves out for example methane and acetone. The machine also leaves residue from the previous samples in the tubes, which means contamination of the next sample is possible.

3.4 Thermogravimetric analysis - TGA

The TGA reveals the decomposition range and the evaporation rate. In this thesis, the matter of interest is the decomposition range where the different crosslinkers are used and the relation to the curing time. Normally, a XLPE will have a decomposition range between 400 – 500°C.

Samples for the TGA are extracted from the middle of the genuine cable sample from the pilot machine with a knife. The samples were tested using a temperature ramp set to 600°C. The TGA samples are made in alumina sample holders, with an average of 12 mg of polymer. The heating rate was 10°C/min and the test was performed under a nitrogen gas flow of 100 ml/min.

3.5 Structure analysis - FTIR

Fourier Transform Infrared Ray, FTIR, was used to measure the structure, in the wavenumber range of 4000 – 400 cm^{-1} , of a solid sample. The FTIR samples used were from the genuine crosslinked samples from the pilot machine. The FTIR samples were carved out from the center of the extruded insulation with a knife. The aim was to observe specific bonds that were a result from the crosslinking and compare to non-crosslinked samples.

3.6 Differential scanning calorimeter – DSC

A differential scanning calorimeter (DSC) will measure the heat flow through a sample in a pan, heat flow in and out of a sample versus its temperature, which will give the thermal characterization of the material. The change in enthalpy tells whether the change in the material is an endothermic or exothermic change, which can be related to melting or crystallization respectively. To get rid of the thermal history of the sample, a cyclic program is needed. A typical cyclic program on a DSC uses the format heat – cool – heat. From the heating the melting peak, T_m , is achieved and by integrating the curve the enthalpy for the crystals present are obtained, which gives the crystallinity of the sample. As the cycle continues with cooling, the temperature of crystallization, T_c , is obtained.

The glass transition temperature, T_g , is also obtainable, but it is less relevant for this research. Since the material is not completely amorphous, the T_g will be difficult to find.

The crystallinity of the sample is calculated according to Equation 1. The enthalpy obtained from the melting peak, ΔH_m , is used. The heat of fusion of a 100% crystalline PE (ΔH_0) is 287.3 J/g. [20]

$$X = \frac{\Delta H_m}{\Delta H_0} \cdot 100\% \quad \text{Equation 1}$$

The heating program used in this thesis was taken from the Borealis patent description. [8] For the peroxide-containing products, the temperature was first ramped up from 30 °C to 130 °C, 10 °C/min. Then the temperature was kept at 130 °C for 2 minutes. After the isothermal stage temperature was ramped, 10 °C/min, from 130 °C to 50 °C, where it was kept isothermally again for 2 minutes. The last ramp was from -50°C to 220°C at a rate of 10 °C/min. For the other samples, the steps are the same but the first heating cycle goes up to 180 °C.

Note that the crystallinity of a pure LDPE is higher than for XLPE from the same base polymer. This is due to the increase of crosslinks, which restrict the polymer's chain mobility to form crystals [21]. DSC Samples are taken from genuine samples made at Maillefer Extrusion Oy pilot machine.

3.7 Crosslinking rate - Rheology

With crosslinking rate, the duration for a fully crosslinked sample is measured. Crosslinking time affects the process speed and is, therefore, a big part of the production. The time of crosslinking was investigated with a rheology measurement device. Rheology is the science of a matter's ability to flow and deform. A rheology measurement will therefore give information about how the flow or deformation changes according to different parameters, for instance increasing temperature or with time. In the case of crosslinking of a polymer the interesting part is time, since as the crosslinking proceeds, viscosity will change. There will be a material-specific point that will show on the graph

where the crosslinking starts and it can be estimated where it ends when the slope is close to zero, meaning the material is fully crosslinked. [22]

A rheometer is used to measure the response of a liquid, plastic or rubber, as a force is applied. The rheological behavior tells much about the structure of the material and the progress of the crosslinking can be clearly seen. The force applied creates a shear stress (τ) in the material, which then creates a deformation in the material, referred to as the shear strain (γ), see Figure 13. Often a constant strain is applied and the shear rate ($\dot{\gamma}$) over time is measured. From this information, by deriving, the storage modulus (G'), loss modulus (G'') and phase angle (δ), as well as the change of viscosity (η), may be calculated.

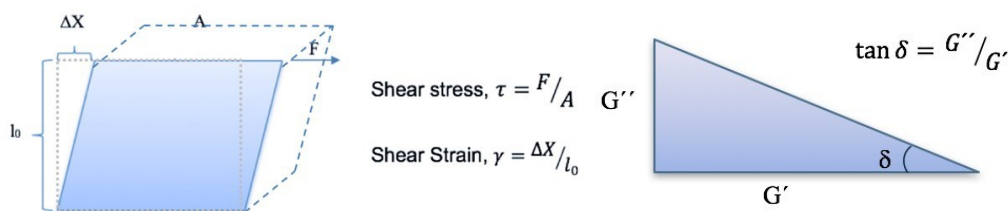


Figure 13. Rheology measurements are based on shear forces applied on a matter.

Figure 14 shows an example of a rheological measurement method called oscillatory sweep, which gives the behavior of storage and loss modulus. The storage modulus tells about the stored energy and elasticity (if it is a solid, the dampening behavior) of a material and the loss modulus tells about the energy lost by heat (viscose response). It can clearly be seen from Figure 14 when the material is changing from a liquid to a solid, when G' becomes larger than G'' . This point is called the gel point.

The phase angle, δ , can be determined from the loss and storage modulus according to the following equation, $\tan(\delta) = G''/G'$, where $\tan(\delta)$ is the dampening factor or loss factor of the material. The value of the phase angle tells about the material's viscose appearance; if it is greater than one, the material performs like a liquid and, if less than one, the material preforms like a solid. As the phase angle is based on trigonometric tangent, it will equal zero at 0° , and one at 45° . This means that, if the phase angle is zero, it behaves

like a solid, whereas if one, it behaves like a liquid. Polymers will themselves place in-between and therefore show elastic and viscous behavior at the same time, hence they are called viscoelastic materials. When performing an oscillation measurement, the phase shift in the measured oscillation strain is the same as the phase angle, see Figure 15.

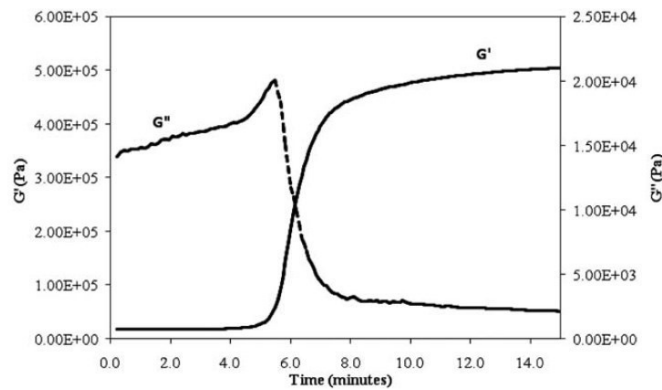


Figure 14. Example of a frequency sweep oscillatory measurement - Storage (G') and loss modulus (G''). [23]

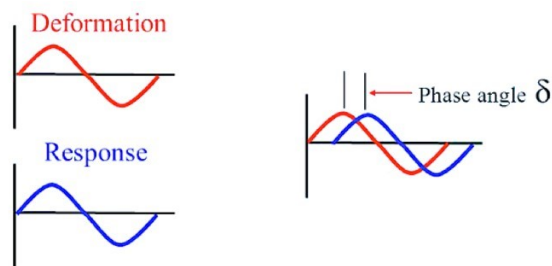


Figure 15. Oscillation measurement showing the correlation between measured strain phase shift and phase angle. [24]

There are several kinds of rheometers and in this work a rotational rheometer was used. A rotational rheometer is measuring shear strain, as the matter is subjected to either constant stress or strain. There are several kinds of geometries used for the measuring head, in this case a plate to plate shearing rheometer was used. The set-up is demonstrated in Figure 16. The measuring head above is rotating or oscillating while the bottom part is the test chamber. The test chamber is an heated enclosure and it is stationary.

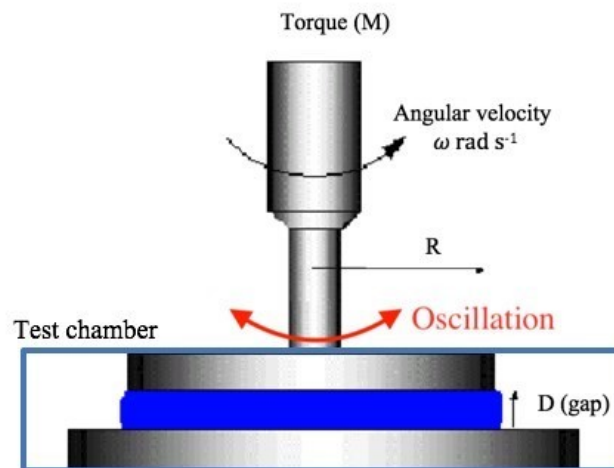


Figure 16. Plate - plate shearing rheometer. Arrow is showing the oscillation motion. [25]

With a rotational rheometer the torque created by the sample is recorded. An oscillatory measurement can be performed as well. Oscillation of the measuring head gives the elastic behavior of the material. In an oscillation measurement, different amplitudes and frequencies can be chosen, either constant or not. These two methods are called amplitude and frequency sweep. The rheometer may also have a heating environment to measure rheological changes in a temperature, for instance the plastic's processing temperature.

In an amplitude sweep, the typical frequency is set at 0.5 rad/sec and the strain varies from 0.1 to 100%. The purpose of an amplitude sweep is to determine the viscoelastic region, which gives a limit to the strain that should not be exceeded when performing a frequency sweep. An amplitude sweep gives the loss and storage modulus plotted against the deformation. At low deformation the storage and loss modulus is constant, meaning that the structure of the sample is not disturbed.

With a frequency sweep the viscoelastic properties of the material are determined. The frequency is changing during the sweep, while the amplitude of the shear stress is kept constant. The result can be plotted as the storage and loss modulus as a function of the frequency. The plot gives information about polymers' glass transition temperature (T_g), melting point (T_m) and material specific characteristics. In a seminar held by G.R. Dr.

Abel, it was claimed that when plotting torque (M) against time (t) the so called vulcanization curve is achieved, see Figure 17.

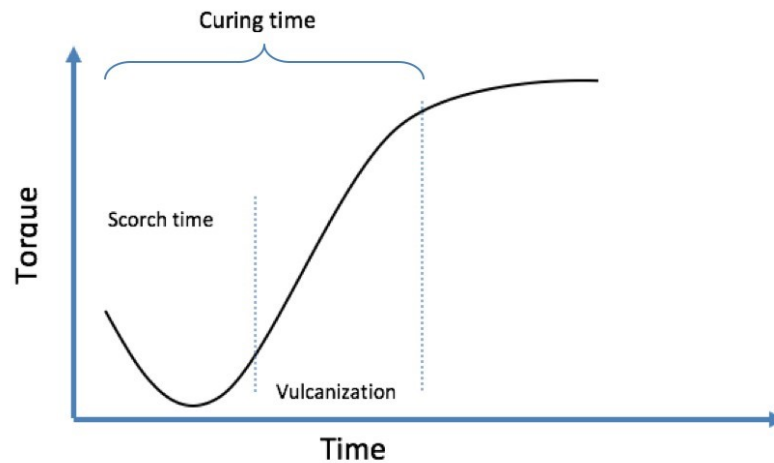


Figure 17. Rheology measurement scheme of the curing time.

The rheology measurement process begins by melting the compounds and creating a good flow. The next stage is where the vulcanization process begins and an increase in torque can clearly be seen. The rate of the increase is referred to as the vulcanization rate. The optimum curing time, t_{90} , is when the curing has reached 90% of the maximum torque. [23] This phenomenon, where the curve plateaus, can be seen in Figure 17, where $\tan(\delta)$ is plotted against time. The same phenomenon is seen in plots with torque against time.

When performing a frequency sweep, the loss and storage moduli and their behavior are achieved. This can be converted to a graph that displays $\tan(\delta)$ against time and from where the three phases, induction, curing and over-curing, can clearly be seen, as in Figure 18. From the figure, a good estimation about the value for t_{90} can also be determined by locating δ_{90} in the graph. The calculation for δ_{90} is shown in Equation 2. In the equation, δ_{\max} and δ_{\min} are the maximum and minimum values of δ . This estimation has been proven in research [23] by Khimi et al. where the results for t_{90} in an oscillating rheometer were compared to a curemeter, which uses a method called Dynamic Mechanical Analysis (DMA). The device gives the most precise measurement of the curing point. The report states that one can determine the correct time for t_{90} with $\pm 5\%$ margins by calculating δ_{90} .

$$\delta_{90} = \delta_{max} - 0.9(\delta_{max} - \delta_{min})$$

Equation 2

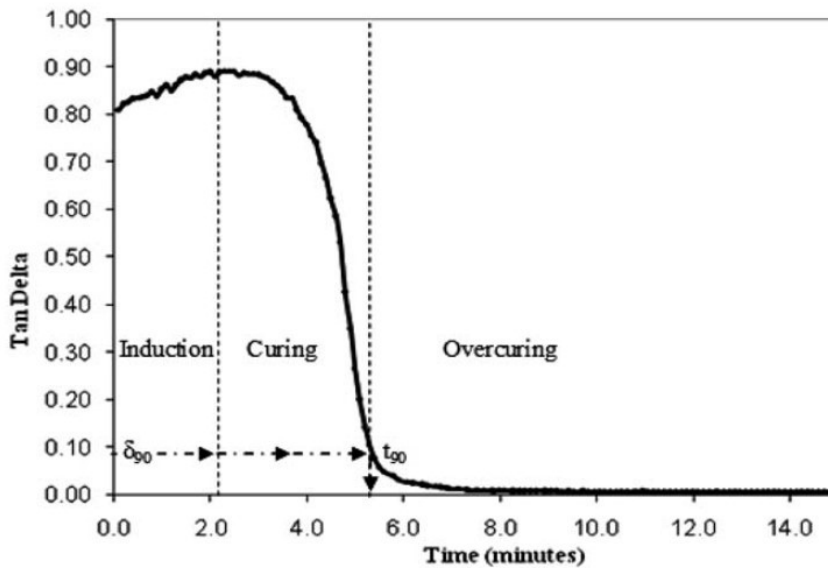


Figure 18. Tan delta with time showing the absolute curing time for a typical thermosetting polymer. [23]

In this research, the crosslinking at certain temperatures is of interest. A method called an isothermal strain sweep is first performed to determine the linear strain region, followed by a time sweep measurement at interesting temperatures using constant strain, γ , and a constant frequency, ω , of the oscillation. The strain and frequency were chosen from the linear region of the strain sweep. This gives the curing curve, from which can be determined when the material has cured. Uncrosslinked laboratory samples were used for these tests.

3.8 Degree of crosslinking - NMR

Another area of interest is the crosslinked network. This is examined with a method using solid-echo ^1H NMR relaxation. The sample is placed into the NMR as a solid piece. The material is subjected to a pulse and then the spin-spin relaxation time of the polymer chains of the amorphous regions are registered. [26]

The test is done on crosslinked samples from the pilot machine. The samples are extracted from the center of the insulation with a knife.

3.9 Conductivity

The conductivity was measured at Tampere University of Technology (TUT). The samples that were sent to TUT are Borealis DC, SILEC and Åbo azo. Borealis DC is used as a reference due to its well-known conductivity and good performance. It is also widely used in the industry.

Samples for the conductivity measurements are made of the crosslinked cable samples from the pilot machine. The cable piece is attached to a lathe and cut 0.2 mm thick and 50 mm wide strands in the direction of the turn. The measured samples are then taken from the center of the insulating part. The samples are degassed before testing in a 60 °C vacuum oven over the weekend.

Resistivity, in ohmmeter ($\Omega \times m$), of a material is measured as the magnitude of the current flowing through a sample. The samples were exposed to three different electrical fields: 10, 20 and 30 kV/mm. The current flowing through the material is not constant in the beginning, hence the actual measurement needs to be done when the current is either evened out through the material or at a certain time after switching on the electrical field.

3.10 Gel content

The gel content of the crosslinked polymer can be determined by a soxhlet extraction. The gel content or fraction of gel, f_{gel} , is an indication of how much of the polymer has crosslinked in percent of the weight. The gel content is calculated using the following equation, Equation 3:

$$f_{gel} = \frac{m_1}{m_2} \times 100 \quad \text{Equation 3}$$

$m_2 = \text{Initial mass}$

$m_1 = \text{final mass}$

The extraction is performed in boiling p-xylene for 24 hours.

3.11 Mechanical properties

From each of the cable samples from the pilot machine, 12 dumbbell tensile test samples were made. Dumbbells are punched with a standard stencil from 2 mm thick sheets that are cut in the axial direction of the cable. The tensile samples are tested in both ambient conditions and at elevated temperatures. The elevated temperature is chosen to 95 °C, due to literature claiming cable temperatures could reach up to 90 – 100 °C when in use. [18]

The sample length is 20 mm with a width of 5 mm and thickness of 2 mm. Machine settings are according to the standard of the dumbbell size used.

4 RESULTS

4.1 Pyro-GC/MS

A pyrolysis GC-MS test was performed to determine byproducts that may occur under production or under degassing of the insulation. The results show many different alkanes, from C6 to C34. The samples also show large peaks of triallyl isocyanurate (TAIC) in sample 1, triallyl cyanurate (TAC) in sample 2 and dibutyl disulfide in sample 3, which were all used as the crosslinking agent in respective sample. Small amounts of TAIC were also found in sample 2, which is probably due to residues left in the instrument from sample 1. Sample 2 also shows di-tert-butyl dicarbonate, di-tertbutylhydrazodicarboxylate and bis(ethylhexyl)phthalate. Sample 2.1 shows almost only TAIC and some large carbon chains. The same applies to sample 1.1, with the exception that isopropyl myristate and bis(ethylhexyl)phthalate show in small quantities.

A pyrolysis GC-MS test was also made on the pure crosslinking compounds and co-agents. The pure crosslinking compounds are integrated in the same table as the laboratory samples. Byproducts observed from the pyrolysis match the expected results to some extent. The byproducts that were missing are the small molecules that would have evaporated too fast for the instrument to pick them up. The decomposition route for the Åbo azo compound can be seen to support the observed substances from the pyrolysis, as illustrated in Figure 19. For the Åbo azo, a cyclohexyl propyl ester was visible which, in theory, should not be possible. This indicates a contamination from previous samples in the machine. The other crosslinkers and co-agents' decomposition routes have been presented earlier.

Table 2. Substances found in py-GC-MS test

Sample	Substances found
0	Alkanes C6-C34
DCP	1-phenyl-1-methylethylene Acetophenone 2-phenyl-2-propanol 1-phenyl-1-ethanone Propiophenone 1-(3-methylphenyl)ethanone
1.1	TAIC Isopropyl myristate Bis(ethylhexyl)phthalate Alkanes C28-C36
1.2	TAIC Alkanes C6-C34
Trigonox 101	Nothing detected
TAIC	2,4,6-tris(allyloxy)triazine
2.1	TAC Di-tert-butyl dicarbonate Di-tert-butylhydrazodicarboxylate Bis(ethylhexyl)phthalate TAIC Alkanes C28-C36
2.2	TAC 2-tert-butylsulfanylacetic acid Di-tert-butylhydrazodicarboxylate TAIC Bis(ethylhexyl)phthalate Alkanes C6-C36

DBAC	Tert-butyl carbamate Di-tert-butylhydrazodicarboxylate Sulfurous acid Butyl isobutyl ester Di-tert-butyl dicarbonate Styrene 3-phenylbut-3-enylbenzene Triallyl cyanurate
TAC	2,4,6-tris(allyloxy)triazine
3.1	Dibutyl disulfide Alkanes C6-C38
3.2	Dibutyl disulfide Alkanes C6-C34
Åbo Azo	1-tert-butylcyclohexane Cyclohexyl propyl ester (Cyclopentylmethyl)cyclohexane 1,1-bicyclohexyl

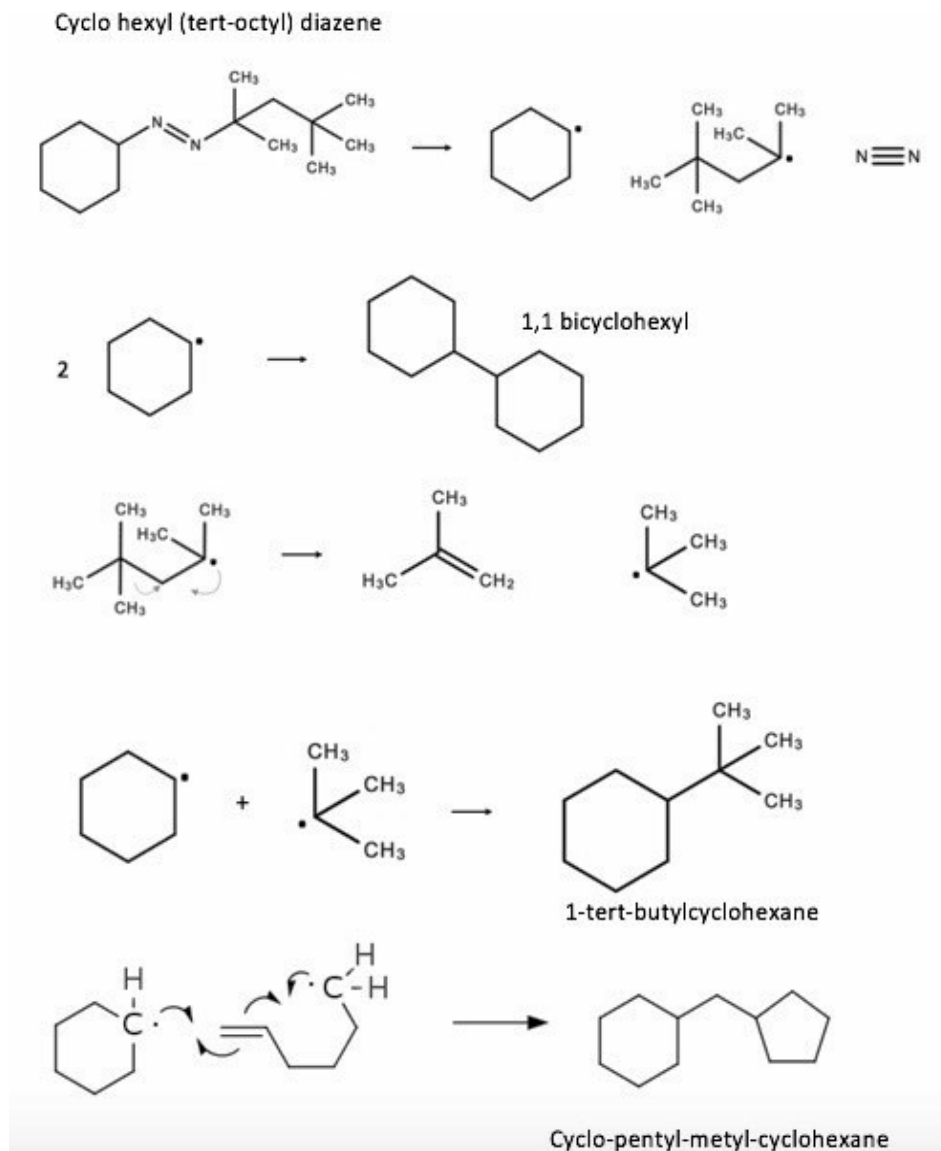


Figure 19. Decomposition products of Ábo azo compound.

4.2 Rheology

The optimum curing times for the different samples tested are presented in Figure 20. From Table 3 can be seen, for each laboratory sample, the type of crosslinker used, the temperature, the approximate gelation point and the approximate time of reaching an optimally crosslinked polymer, t_{90} . t_{90} is determined by looking at the $\tan(\delta)$ and determining the point where it becomes linear or nearly linear. Once the start of the linear region is determined, the optimum curing time can be determined as 90% of the time to reach the linear region, as illustrated in Figure 20.

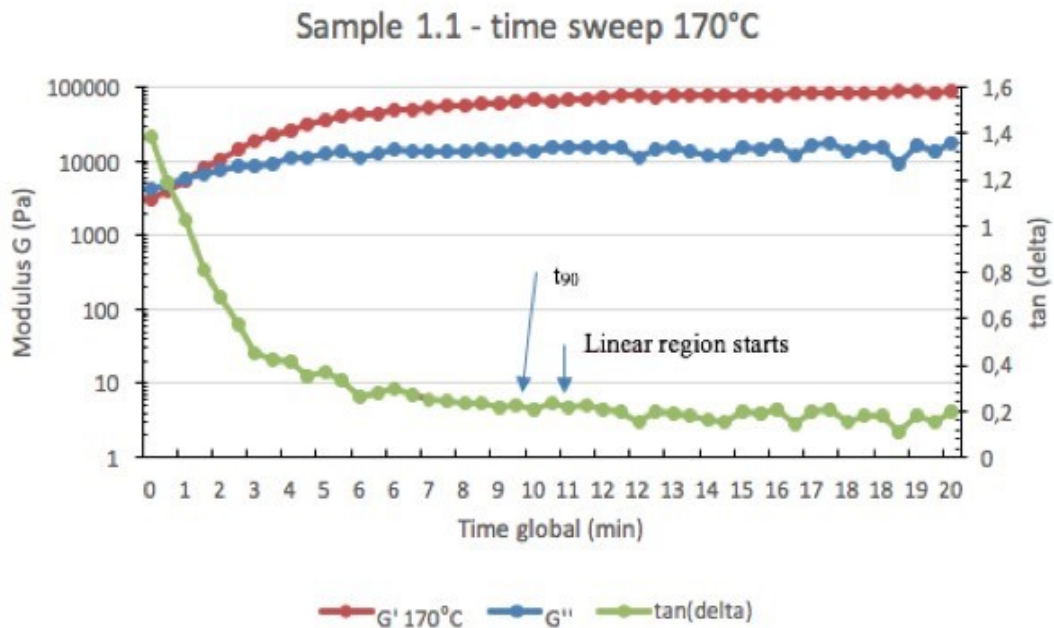


Figure 20. Time sweep of sample 1.1 - How t_{90} is determined.

The reference sample 0, was the fastest, when comparing gelation points to the other samples. When comparing sample 1 with the reference sample 0, the difference in time is however minimal. Samples 2 and 3 were crosslinked with an azo compound, which clearly gave a much longer gelation and curing time at the temperature range of interest. Furthermore, as the optimum curing range should be taken from a temperature ramp diagram, the range appear to be at a higher temperature for sample 2 and 3 than for sample 0 and 1. Sample 0 and 1 clearly have an optimum range at 160°C – 180°C, whereas samples 2 and 3 is in the range of 210°C – 240°C. An example of the temperature ramp diagram can be seen in Figure 21. The minimum viscosity point can be determined from the diagram, which is of interest when determining the optimal processing temperature.

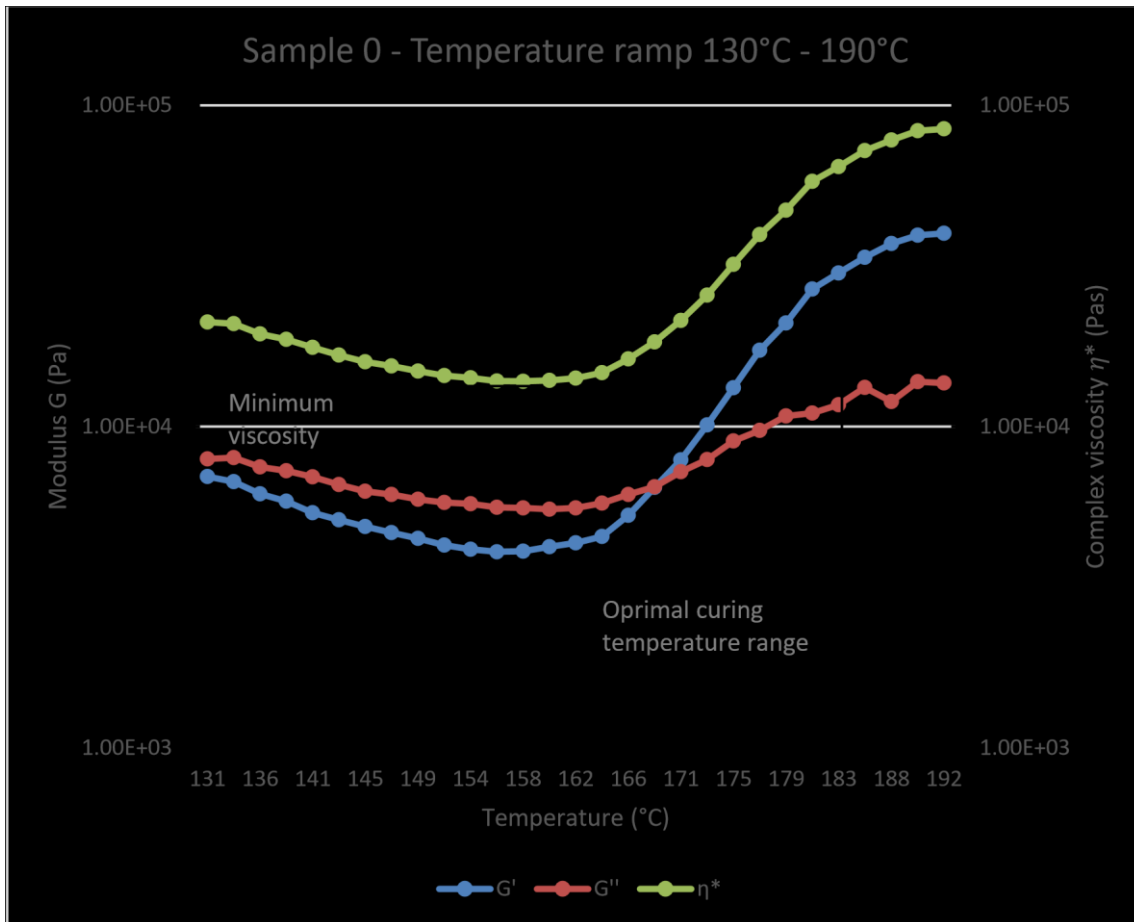


Figure 21. Temperature ramp rheological measurement to determine optimum curing temperature range.

The aim is to find a better or equally good blend as sample 0 in the temperature range of 170 – 190°C. It can be concluded that only sample 1 with the crosslinker Trigonox 101 is close to sample 0. Sample 1.1 is a faster than 1.2, as it has a slightly higher content of crosslinking agents, 1.40 wt% compared to 1.25 wt%. From this can be concluded that the more peroxide, the faster is the crosslinking.

When comparing samples 2 and 3, which are crosslinked with azo compounds, sample 3 appears better. The temperature range of interest is 170 - 190°C, was shown to not be high enough for azo compounds to crosslink at a reasonable time. The temperature ramp reveals the optimum curing range to be at higher temperatures, at temperatures from 210 to 240 °C, where more tests were made. The samples 2 and 3 were only tested at 170°C for the gelation point, since the time to reach optimum crosslinking would be very long. A test for the optimum crosslinking time was however conducted at 190°C. If the trend

from the other samples analyzed, the results indicate that the time is increased by at least four times at 170°C compared to 190°C.

Table 3. Data of the curing time based on rheological dynamic time sweep for different temperatures

SAMPLE	TYPE OF CROSS LINKER	TEMPERATURE	APPROX. GEL POINT	APPROX. T₉₀
0	Peroxide	170	54 s	8.1 min
		180	24 s	2.7 min
		190	< 24 s	0.9 min
1.1	Trigonox 101	170	1 min 18 s	9.9 min
	TAICROS	180	24 s	5.4 min
		190	< 24 s	2.7 min
1.2	Trigonox 101	170	2 min 6 s	11.7 min
	TAICROS	180	1 min	3.6 min
		190	< 24 s	2.7 min
2.1	DBAC	170	76 min	-
	TAC	190	27 min	77.4 min
		220	8 min 6 s	27 min
		230	6 min	25.2 min
		240	4 min 42 s	23.4 min
2.2	DBAC	170	40 min	-
	TAC	190	20 min	50.4 min
2.2		220	3 min 24 s	18.9 min
		230	1 min	18 min
		240	<24 s	11.7 min

3.1	Åbo-Azo	170	66 min	-
	TAC	190	26 min 6 s	53.1 min
		220	6 min 48 s	24.3 min
		230	3 min 24 s	21.6 min
		240	1 min 18 s	18.9 min
3.2	Åbo-Azo	170	63 min	-
	TAC	190	11 min 36 s	77.4 min
		210	2 min 6 s	12.6 min
		220	24 s	5.4 min
		230	<24s	3.6 min

4.3 DSC

The data from the DSC is presented in Figure 22 and Figure 23. The DSC cycle starts with heating, followed by cooling and heating again. The first heating erases the thermal history of the sample. The cool down gives the temperature of crystallization, T_c . The second heating gives the temperature of melt, T_m , from where the crystallinity can be obtained. The crystallinity, as well as T_m , T_c and the onset temperatures are listed in Table 4. The crystallinity is calculated according to Equation 1. Each sample is tested twice from different locations of the genuine cable insulation, both from the center of the insulation.

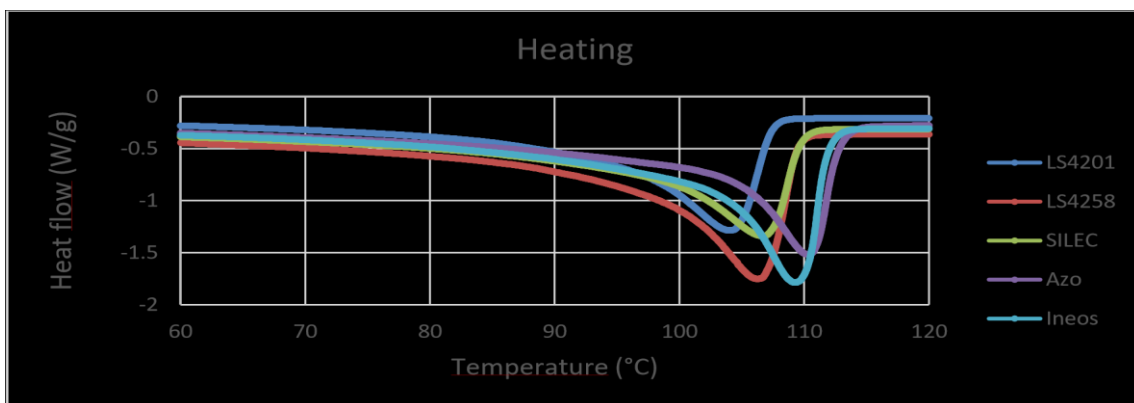


Figure 22. DSC Heating curve of samples from the pilot machine. LS4201 is Borealis AC, LS2458 is Borealis DC samples.

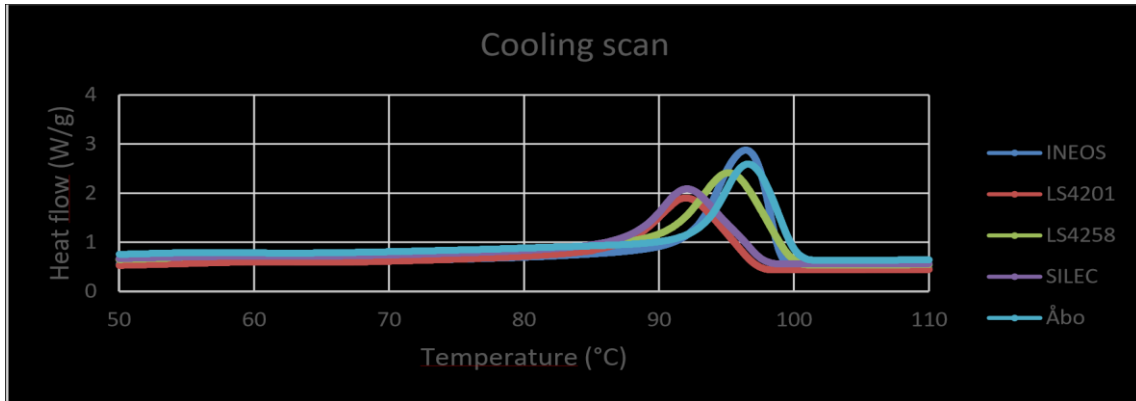


Figure 23. DSC cooling curves of samples from the pilot machine. LS4201 is Borealis AC, LS2458 is Borealis DC samples

Figure 22 and Figure 23 show heating and cooling curves. From the heating curve it can be seen that the melting temperatures of the samples differ from each other. The melting temperature should increase as the degree of crosslinking increases, as the structure reduces flexibility of the chains. The higher the degree of crosslinked is, the lower will the enthalpy of fusion be, which in turn leads to a lower crystallinity. The crystallinity was concluded from the data and the results, in order of decreasing crystallinity, are Ineos, Borealis DC, Borealis AC, SILEC and Åbo azo.

Table 4. DSC data obtained from graphs

Sample	T _m (°C)	T _{om} (°C)	T _c (°C)	T _{oc} (°C)	Crystallinity
Ineos	109.2	101.8	96.4	99.1	46.9%
Ineos (2)	108.9	102.3	96.8	99.3	41.6%
Borealis DC	106.3	96.0	95.2	99.8	49.4%
Borealis DC (2)	107.4	95.5	94.1	99.6	41.4%
Borealis AC	103.7	93.0	92.2	97.4	45.6%
Borealis AC (2)	104.0	92.4	92.1	97.2	38.7%
SILEC	106.6	95.2	92.1	97.6	32.6%
SILEC (2)	108.1	94.2	90.75	97.2	46.0%
Åbo Azo	110.1	102.6	97.2	100.4	38.5%
Åbo Azo (2)	110.3	102.6	96.6	100.1	37.0%

4.4 FTIR

From the FTIR spectra information is obtained about the bonds formed from the crosslinking. The samples with different crosslinking agents are compared to the clean LDPE. An example of a clean basepolymer, Ineos BDP-2000, is shown in Figure 24.

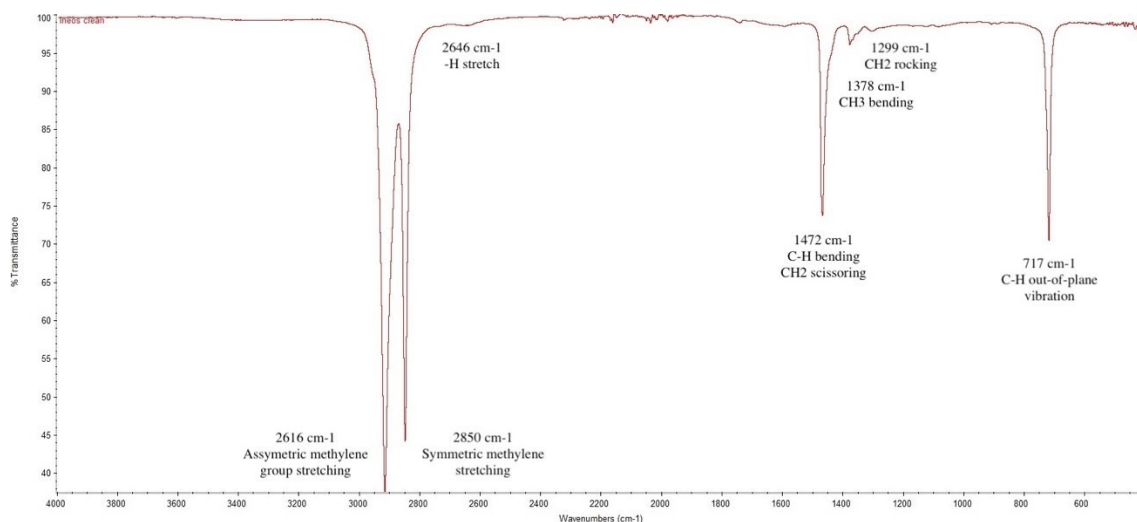


Figure 24. Ineos BDP - 2000 FTIR

All samples have the typical spectra for polyethylene, when matching the spectra with the database. The typical line for polyethylene gives a strong peak for methylene stretching at 2916 and 2850 cm^{-1} . Other typical peaks at 1472 and 717 are C-H bending, scissoring and vibrations.

The analysis of the FTIR is focusing on the presence of double bonds that could be vinyl groups or ketones. The presence of vinyl groups affects the crosslinking according to reference [27] and is therefore of interest. No polar products should exist in the insulation. Vinyl groups give signals at 909 and 990 cm^{-1} , of which 909 cm^{-1} is the stronger signal. A ketone gives a signal at slightly above 1700 cm^{-1} . Vinyl groups should be appearing in every sample that is not crosslinked. As the crosslinking reaction proceeds, the double bonds should be consumed.

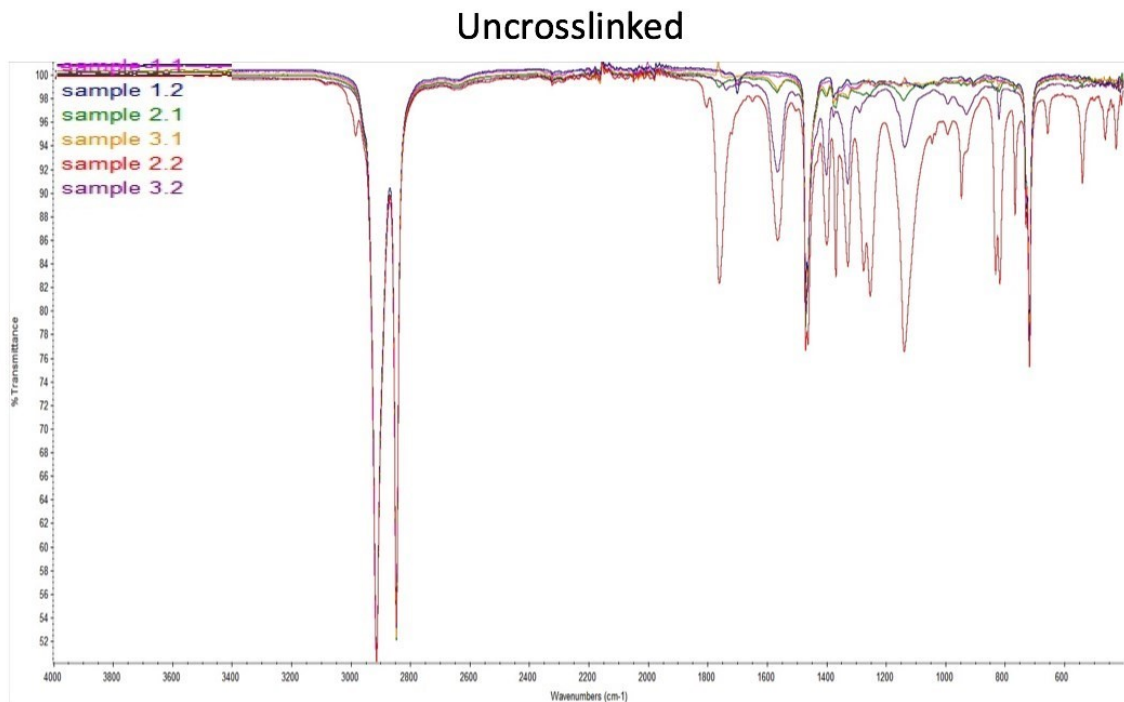


Figure 25. FTIR spectra of all non-crosslinked laboratory samples.

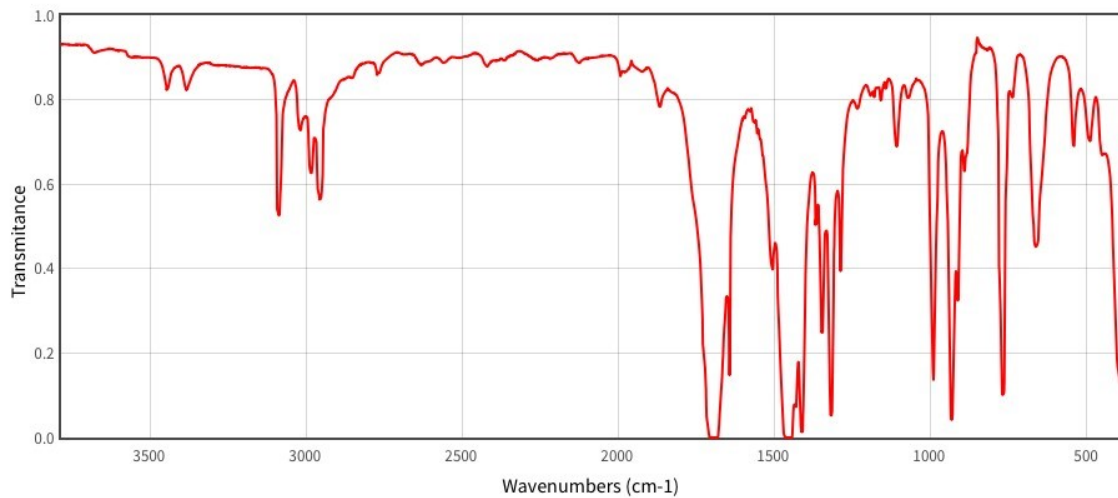


Figure 26. Triallyl isocyanurate (TAC) FTIR spectra. [28]

Figure 25 show the spectrums of the non-crosslinked samples. Samples containing peroxides are not showing any strong peaks, unlike the red and purple samples which contains azo crosslinkers. The crosslinking aid TAC that is used with azo samples 2 and 3 show several strong peaks in the region $1700 - 500 \text{ cm}^{-1}$. It clearly shows peaks for vinyl groups and ketones. As a reference, the IR spectra of TAC is shown in Figure 26, which can be related to the samples containing TAC. The more TAC in the sample, the more clearly it shows.

The samples shown in Figure 27 are crosslinked samples from the pilot machine. It is clear that many of the vinyl groups and ketones are consumed during the crosslinking. However, Åbo azo leave a few peaks here and there that indicate that there are many compounds in the matrix, which is not present in the other samples. The Åbo azo and Borealis AC cable grades are very similar, both containing many more peaks than the DC cable grade and the SILEC sample.

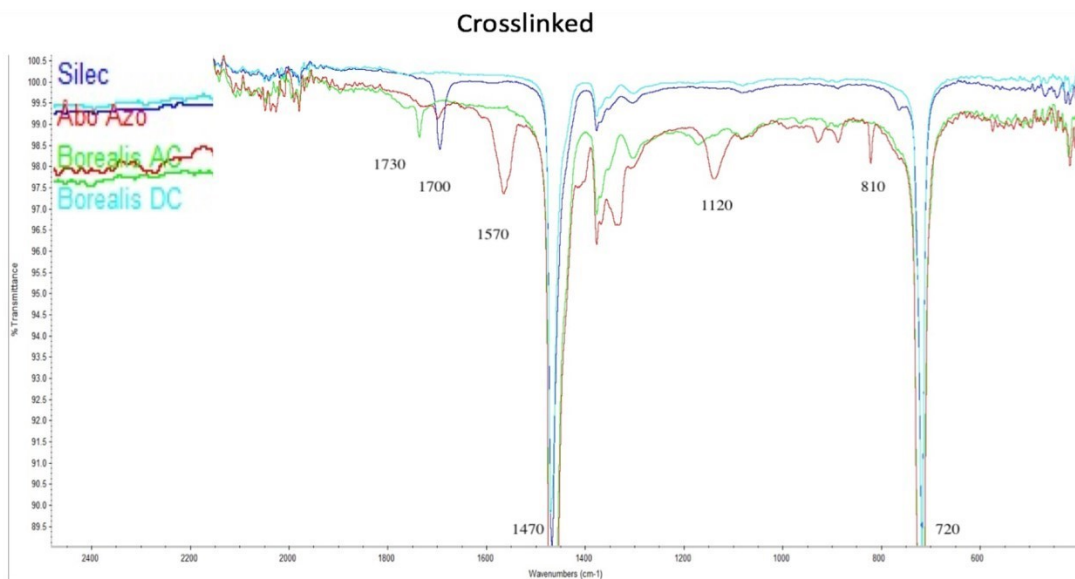


Figure 27. FTIR of genuine cable samples from the pilot machine.

The FTIR in Figure 27 are cut from 2400 – 600 cm^{-1} , since the spectra of the samples will only differ in this region. The Sigma-Aldrich IR spectrum table and chart is used to determine the functional groups for signal peaks found in the spectra. The figure shows that Borealis DC is very flat compared to the others, meaning it contains no significant extra bonds or functional groups. The SILEC sample is similar, except from a clear peak at 1700 cm^{-1} that appears to be a C=O stretch from a conjugated aldehyde. The two significant peaks at 1470 cm^{-1} and 720 cm^{-1} are the fingerprint of an LDPE, as seen from Figure 24 of the clean base polymer. Borealis AC looks clean as well, apart from the stretching at 1730 cm^{-1} , which is an aldehyde C=O stretch as well.

The Åbo azo appears to have many peaks and bonds that are stretching and vibrating. This is probably due to the TAC used as a crosslinking aid. A large peak is visible at 1620–1550 cm^{-1} which could be a combined peak due to the bulkiness of it, but is also the region for an N-H amine bend or a C=C cyclic alkene stretch. The Åbo azo also has a C=O conjugated aldehyde stretch at 1700 cm^{-1} . The following noticeable peak is at 1120 cm^{-1} , which could be a C-O aliphatic ether stretch or a C-N amine stretch, or even both. The peaks appearing at 900–700 cm^{-1} are signals from C-H bending. [29]

4.5 NMR

A method using the NMR signals to determine the relaxation of PEX is performed. The reference for this method is described in reference [30]. A solid echo experiment was performed and the results are presented in Figure 28. The denser the crosslinking is, the faster the material will relax. It can be seen in Figure 28 that LS4258 has the tightest network with the shortest relaxation time, whereas the Åbo azo has the loosest with the slowest relaxation time. LS4201 and SILEC are quite similar, but LS421 has a slightly faster relaxation and tighter network. All in all, the materials are very similar.

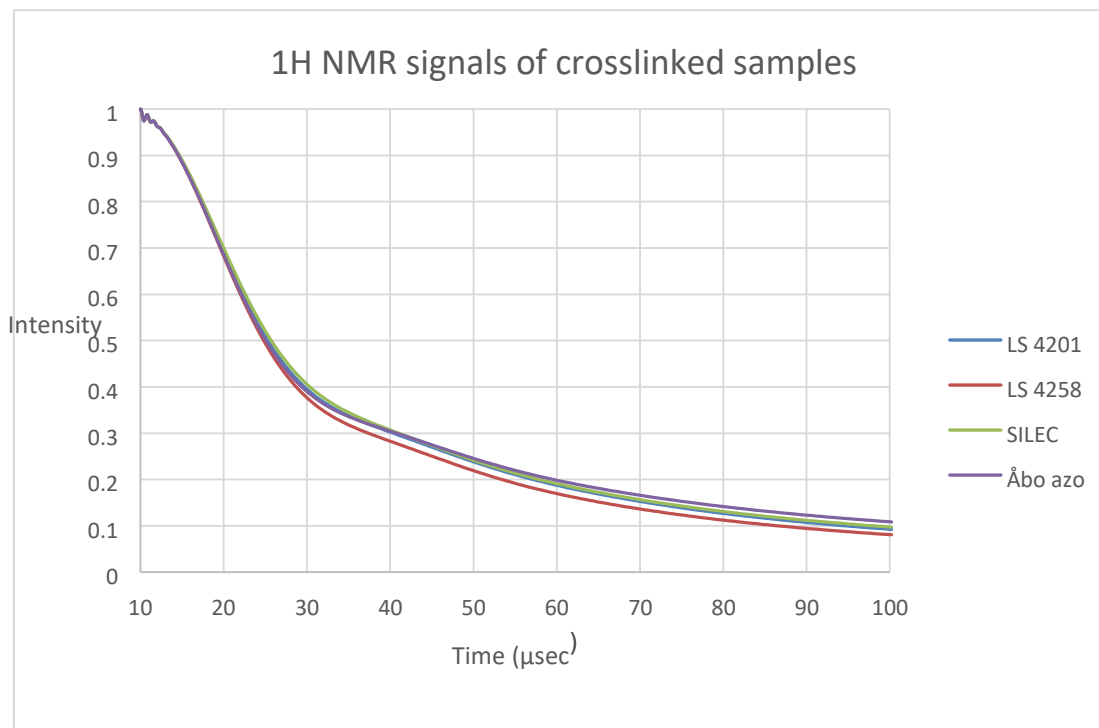


Figure 28. 1H NMR solid echo experiment run on the different samples made at the pilot machine. LS4201 is Borealis AC, LS2458 is Borealis DC samples.

4.6 Gel content

The samples were boiled in p-xylene for 24 hours. The results are presented in Table 5. The results are questionable, due to the reference sample, INEOS, that should have completely dissolved, did not dissolve completely. This indicates that the extraction did not work as expected.

Table 5. Soxhlet extraction results giving the gel content of the genuine cable samples from the pilot machine.

SAMPLE	M₁ (G)	M₂ (G)	F_{GEL} (WT%)
Borealis DC	1.4631	1.0399	71.1
	0.9926	0.6526	65.7
	1.0405	0.6990	67.2
	0.9431	0.6735	71.4
Borealis AC	1.8847	1.6075	85.2
	2.3926	2.0938	87.5
	1.5506	1.3505	87.1
SILEC	1.8077	1.4952	82.7
	2.2771	1.8885	82.9
	1.2212	1.0630	87.0
ÅBO AZO	1.0984	0.8373	76.2
	0.9406	0.7635	81.2
	1.0724	0.8984	83.8
INEOS	0.9150	0.8216	89.8

4.7 Tensile test

Tables 6 and 7 shows the tensile strength of all samples in room temperature and 95°C respectively. Each sample was tested 6 times and the value in the table is the mean value of all six tests. Figure 29 visually illustrates the results.

Table 6 Mechanical properties of all samples in room temperature. LS4201 is Borealis AC, LS2458 is Borealis DC.

Sample	Young's modulus (MPa)	Elongation at beak (%)	Tensile strength (MPa)
LS 4258	15.24	985	31.8
LS 4201	12.78	867	29.3
SILEC	11.85	762	30.6
Åbo azo	15.19	888	24.1

Table 7. Mechanical properties of all samples in 95°C. LS4201 is Borealis AC, LS2458 is Borealis DC.

Sample	Young's modulus (MPa)	Elongation at beak (%)	Tensile strength (MPa)
LS 4258	1.78	<250 mm	10.4
LS 4201	1.77	724	7.3
SILEC	1.88	487	6.1
Åbo Azo	2.44	1198	7.5

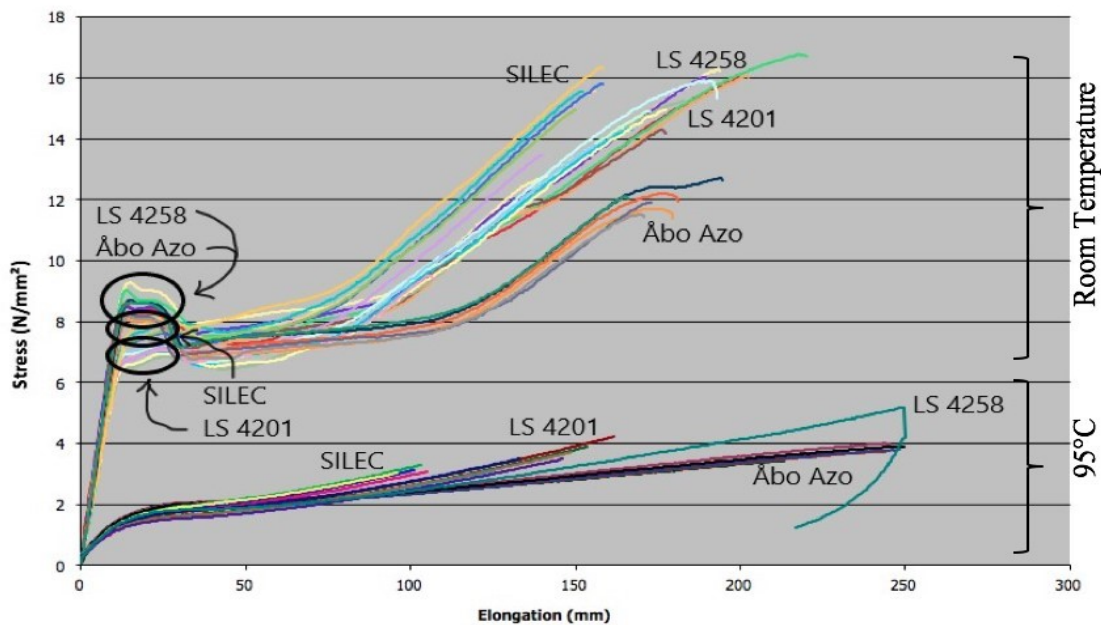


Figure 29. Tensile test data of all samples in a stress - strain diagram. LS4201 is Borealis AC, LS2458 is Borealis DC.

From figure 29 can be seen the different samples mechanical properties in a stress – strain diagram. The upper curves are tests at room temperature (23 °C) and the lower curves are

tests at 95 °C. In the room temperature samples, it can be seen that the yield strength is highest for LS 4258 (Borealis DC) and Åbo azo, while it is weakest for LS 4201 (Borealis AC) and SILEC. The differences are not large, but still noticeable. The weakest being around 7 MPa and the strongest 9 MPa. Åbo azo has the weakest stress at fracture, around 12 MPa, but maintaining a longer linear necking region before rupture compared to the other samples. It could be due to the crosslinking network being looser and therefore easier for the chains to untangle, leading to more elongation. LS 4258 (Borealis DC) and SILEC have the highest stress at fracture, about 15 MPa. LS 4201 (Borealis AC) has a stress at fracture of 14 MPa.

When the temperature rises to 95 °C, it evens out the strain hardening region to a smooth curve. The yield point has decreased for all samples to about 1.5 MPa. The elongation of the SILEC samples was reduced from 762% to 487% and the same applies to LS 4201 (Borealis AC) that had reduction from 867% to 724%. Åbo azo and LS 4258 (Borealis DC) have had an increase in elongation, where Åbo azo increased from 888% to 1198% and LS 4258 (Borealis DC) did not break at all until the maximum limit on the tensile machine was reached.

4.8 Conductivity

Conductivity measurements were performed on the Borealis DC, SILEC and Åbo azo genuine cable samples. During the experiment it was noticed that the current flow was not evening out on all samples, hence it was instead measured at a constant duration – 10 000s. Samples were tested at 60 °C. The results are presented in Table 8 and illustrated in Figure 30.

Table 8. Resistivity results measured at 60°C

Sample	Resistivity [$\Omega \times m$]		
	10 kV/mm	20 kV/mm	30 kV/mm
Borealis DC	$1.50 * 10^{14}$	$7.96 * 10^{14}$	$3.04 * 10^{14}$
SILEC	$8.21 * 10^{14}$	$1.15 * 10^{14}$	$3.29 * 10^{14}$
Åbo azo	$2.38 * 10^{13}$	$7.68 * 10^{12}$	$7.96 * 10^{11}$

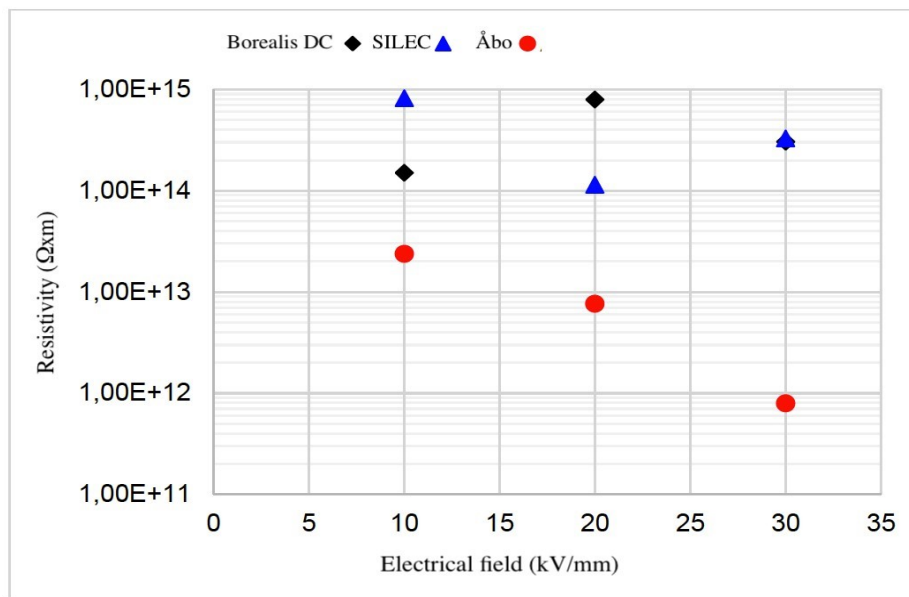


Figure 30. Resistivity measurements of Borealis DC, SILEC and Åbo azo samples exposed to three different electrical fields.

It is clear that the Borealis DC and SILEC samples have the same level of resistivity, whereas the Åbo azo have lower resistivity and becomes even worse as the electrical field is increased. In conclusion, the Åbo azo conducts better, which is undesirable for this purpose.

5 CONCLUSIONS AND SUMMARY

Samples used in the thesis were prepared both in a laboratory melt mixer and genuine cable samples at Maillefer Extrusion Oy's pilot machine. From the samples prepared in the laboratory at Åbo Akademi University, information related to the crosslinking rate and temperature profiles for crosslinking of various cable formulations were obtained. A Borealis grade for a DC cable, containing the initiator dicumyl peroxide (DCP), was used as a reference.

The challenges associated with the crosslinking of LDPE with the DCP initiator is the formation of polar byproducts. Such products are acetophenone and cumyl alcohol and the products impair with the electrical insulating properties. Byproducts in the material cause space charge formation and increase the conductivity of the insulation material. Azo alkanes do not form such detrimental byproducts during the crosslinking process of LDPE. Therefore, two different azo compounds were evaluated as alternative crosslinking initiators to DCP. The azo compounds evaluated were DBAC, that is according to a recipe by ABB, and an azo compound designed and synthesized by Åbo Akademi University.

The selected initiators were analyzed using the pyrolysis GC/MS instrument in order to determine the decomposition products that are formed. Mechanism of their formation is confirmed theoretically. The results confirm that the DCP initiator form decomposition byproducts such as 1-phenyl-1-methylethylene, acetophenone, 2-phenyl-2-propanol, 1-phenyl-1-ethanone, propiophenone and 1-(3-methylphenyl)ethanone. DBAC, which is an azo-carbonyl compound produces mainly the non-polar derivatives tert-butyl carbamate, di-tert-butylhydrazodicarboxylate, styrene, 3-phenylbut-3-enylbenzene as well as some polar derivatives such as butyl isobutyl ester, di-tert-butyl dicarbonate and triallyl cyanurate. The Åbo azo gives rise to mainly non-polar byproducts such as 1-tert-butylcyclohexane, cyclopentylmethyl-cyclohexane and 1,1-bicyclohexyl. The mechanism of their formation is depicted in Figure 19.

Rheometry of the materials are measured with an oscillating disc measurement at elevated temperatures using non-crosslinked laboratory samples in order to determine the time to

completion of crosslinking. Also values for t_{10} and t_{90} is obtained, which is the starting point of curing and the completed curing time respectively. This information was used for the experiments at the pilot machine. The results reveal that both peroxides DCP and Triganox 101 cure rapidly, within 2.7 min and 5.4 min at 180 °C, respectively. It was found that the azo initiators required much longer times for curing than peroxides, up to 30 minutes. Therefore, the temperature had to be raised from 180 °C to 230 °C in order to achieve competitive curing times for the azo compounds.

DSC tests gave the heating and cooling curves of the different genuine cable samples from the pilot machine. The degree of crystallinity should have been the least for Borealis DC, since it is known to have a tight and well crosslinked network. It is known that the Borealis DC material contains less peroxide than SILEC and Borealis AC samples. Borealis AC and SILEC samples have about the same amounts of peroxide by wt%. It is concluded that the more peroxide, the higher the degree of crosslinking is in the sample. Every sample was tested twice, with the samples taken from on different locations of the insulation. There was a huge difference between samples extracted from the same genuine cable sample, indicating that the results are unreliable. Based on the results obtained, the degree of crosslinking was highest for the Åbo azo, followed by SILEC, Borealis AC, Borealis DC samples and the base polymer, Ineos, was as expected the least crosslinked.

Another method for analyzing the density of the crosslinked structure was with a solid-echo ^1H NMR relaxation test. The results were a signal intensity curve as a function of time that shows how fast the polymer is relaxing after a disturbance in the network. The faster the recovery of the structure, the tighter the network. The tightest network is obtained for Borealis DC, followed by Borealis AC, SILEC and Åbo azo. The results conflict with earlier statements; Borealis DC should be less crosslinked than Borealis AC and SILEC. However, the network of Borealis DC appears to be stiffer according to the results.

The results of the extraction with p-xylene gave inconclusive results for the gel content. It was expected that the virgin non-crosslinked LDPE samples would dissolve, but did not.

The FTIR spectral analysis was made for the genuine cable samples. The Borealis DC sample showed no significant number of functional groups that would impart the electrical properties of the DC cable, whereas the SILEC and Borealis AC samples showed an absorbance signal corresponding to C=O stretching. Apart from a strong absorbance signal of C=O stretching in the Åbo azo sample, as well it, obtained several peaks of stretching and vibration of amines, C=C alkenes and C-O ethers. The extra absorbance peaks can be attributed to the presence of unreacted TAC in the sample.

The mechanical strength of the samples was recorded at both ambient conditions and at an elevated temperature of 95 °C. In room temperature, the genuine cable sample containing the Åbo azo initiator had comparable properties with the Borealis DC sample. The Åbo azo sample obtained the highest Young's modulus of 15 MPa of all samples in this study. All samples were very ductile, having an elongation of 800-900%. Borealis DC, Borealis AC and SILEC all showed to have a higher tensile strength of around 30 MPa compared to Åbo azo with only 24 MPa. When the temperature was increased, the Åbo azo sample had the highest Young's modulus of 2.4 MPa, whereas the others had 1.7MPa. The elongation at elevated temperatures was increasing for Borealis DC and Åbo azo, whereas the elongation was remarkably decreased for Borealis AC and SILEC. In the elevated temperature, the tensile strength was the highest for Borealis DC with 10.4MPa and followed by Åbo azo with 7.5MPa. All in all, the performance of the Åbo azo sample in terms of mechanical properties under the investigated conditions matched quite well that of the Borealis DC insulation, which looks promising for the new azo initiator.

The electrical insulation properties of the crosslinked LDPE material for an HVDC cable are of highest importance. Therefore, the resistivity of the genuine cable samples Borealis DC, SILEC and Åbo azo was measured. The tests were done with the electrical fields 10 KV, 20 KV and 30 KV. The Borealis DC conductivity was 10^{-14} S/m at 10 KV and SILEC had a similar value. Åbo azo, in contrast, had over one magnitude higher conductivity, ranging from 10^{-13} to 10^{-11} S/m. The fact that the Åbo azo sample is more conducting is certainly due to unreacted TAC. The existence of residual TAC was confirmed by FTIR analysis.

To finalize, the results showed that a high voltage cable insulation can be successfully prepared using the new azo compound made at Åbo Akademi University. The ABB patent already outlined that the use of azo compounds for high-voltage cable insulation show no polar byproducts from the crosslinking process. However, more research is certainly still required to optimize the azo initiator to polymer ratio and the structure of the azo compound. The use of crosslinking aid, as TAC, should be considered to be replaced by a completely hydrocarbon derivative.

REFERENCES

- [1] G. Mazzanti and M. Marzinotto, *Extruded Cables for High-Voltage Direct-Current Transmission*, John Wiley & Sons, 2013.
- [2] SpecialChem SA, "Omnexus," [Online]. Available: <https://omnexus.specialchem.com/polymer-properties/properties/volumeresistivity>. [Accessed 21 March 2018].
- [3] G. Dominguez, A. Friberg and A. Jedenmalm, "Insulation system for HVDC electrical insulation and an HVDC device having an insulation system for HVDC electrical insulation". Patent WO2014000821 (A1), 3 January 2014.
- [4] M. Marelli, *Achievement and experience in service of long length HV DC electrical links by insulated power cables*, Foz do Iguaçu: Jicable, 2013.
- [5] B. Damsky, "Primer on transmission: AC vs. DC," *Electric Light & Power*, vol. 80, no. 6, 6 January 2002.
- [6] N. Hussin and G. Chen, "Analysis of Space Charge Formation in LDPE in the Presence of Crosslinking Byproducts," *IEEE Transactions on Dielectrics and Electrical Insulation*, vol. 19, no. 1, February 2012.
- [7] J.-O. Bostroem, P. Carstensen, A. Gustafsson, A. Farkas, A. Ericsson, B. Gustafsson, U. Nilsson and C. Fred, "An electric DC-cable with an insulation system". Patent WO 1999033069 A1, 1 July 1999.
- [8] V. Englund, P.-O. Hagstrand, U. Nilsson, A. Smedberg, J.-O. Boström, A. Farkas and G. Dominguez, "POLYMER COMPOSITION FOR W&C APPLICATION WITH ADVANTAGEOUS ELECTRICAL PROPERTIES". Patent US2013081854 (A1), 4 April 2013.
- [9] A. Smedberg, V. Englund, P.-O. Hagstrand, V. Eriksson and E. Silfverberg, "A new crosslinked polymer composition, structured layer and cable". Patent WO2016026878 (A1), 25 February 2016.

- [10] C.-H. HO, E. LOGAKIS, C. Ghoul and A. Krivda, "Chemically cross-linked polyethylene used for electrical insulation". France Patent WO2014075726A1, 15 November 2012.
- [11] University of Southern Mississippi, "Polymer Science Learning Center," Department of polymer science, 2000. [Online]. Available: <http://pslc.ws/macrog/crystal.htm>. [Accessed April 2018].
- [12] S. Nilsson, "The Effect of Crosslinking on Morphology and Electrical Properties in LDPE Intended for Power Cables," Gothenburg, 2010.
- [13] H. Andersson, "Crosslinking of Polymers - Molecular Structure and Properties of Sol and Network," Doktorsavhandlingar vid Chalmers tekniska högskola, Göteborg, 2004.
- [14] S.-S. Choi and Y. Y. Chung, "Considering factors for analysis of crosslink density of poly(ethylene-co-vinyl-acetate) compounds," *Polymer Testing*, vol. 66, pp. 312318, January 2018.
- [15] J. Morshedian and P. M. Hosseinpour, "Polyethylene Cross-linking by Two-step Silane Method: A Review," *Iranian Polymer Journal*, vol. 18, pp. 103-128, February 2009.
- [16] A. Smedberg, T. Hjertberg and B. Gustafsson, "Crosslinking reactions in an unsaturated low density polyethylene," *Polymer*, vol. 38, pp. 4127-4138, 1997.
- [17] A. Thitithammawong , C. Nakason, K. Sahakaro and J. Noordermeer, "Effect of different types of peroxides on rheological mechanical and morphological properties of thermoplastic vulcanizates based on natural rubber/polypropylene blends," *Polymer testing*, vol. 26, pp. 537-546, 5 February 2007.
- [18] J.-C. Gard, I. Denizet, M. Mammeri, B. Poisson, F. Lesage and J. Magnol, "Method for manufacturing a power cable and cable manufactured by means of such a method". France Patent US 20150221419A1, 2 March 2015.

- [19] M. Aubert, R. Nicolas, W. Pawelec, C.-E. Wilen, M. Roth and R. Pfaendner, "Azoalkanes - novel flame retardants and their structure-property relationship," *Polymer for advanced technologies*, pp. 1529-1538, 29 January 2010.
- [20] L. Li, K. Zahng, L. Zhong, J. Gao, M. Xu, G. Chen and M. Fu, "Treeing phenomenon of thermoplastic polyethylene blends for recyclable cable insulation materials," *AIP Advances*, February 2017.
- [21] G. Hossein, "Characterization of conduction and polymerization properties of HVDC cable XLPE insulation materials," Universitetservice US AB, Stockholm, 2018.
- [22] G. M. Thomas, *The Rheology Handbook*, 4th edition ed., Hanover: Vincentz Network.
- [23] S. R. Khimi and K. L. Pickering, "A new method to predict optimum curing time of rubber compound using dynamic material analysis," *Journal of Applied Polymer science*, September 2013.
- [24] G.-R. Dr. Abel, "Fundamentals of Rheology Seminar," 2004.
- [25] K. M. Anal and J. Sehoon, "Using cement paste rheology to predict concrete mic design problems: Tehcnical report," *ResearchGate*, July 2009.
- [26] H. Uehara, T. Aoike, T. Yamanobe and T. Komoto, "Solid state 1H NMR relaxation analysis of ultra high molecular weight polyethynele reactor powder," *Macromolecules*, no. 35, pp. 2640-2647, 2002.
- [27] L. Andersson and T. Hjertberg, "The effect of Different Structure Parameters on the Crosslinking Behaviour and Network Performance of LDPE," Gothenburg.
- [28] NIST Standard Reference Data, "National Institute of Standards and Technology," 2011. [Online]. Available: <https://webbook.nist.gov/cgi/cbook.cgi?ID=C1025156&Mask=80>. [Accessed December 2018].

- [29] Merck KGaA, "Merck (Sigma-Aldrich)," [Online]. Available: <https://www.sigmaaldrich.com/technical-documents/articles/biology/ir-spectrumtable.html>. [Accessed 14 December 2018].
- [30] U. Hiroki, A. Taku, Y. Takeshi and K. Tadashi, "Solid-State ^1H NMR Relaxation Analysis of Ultra Molecular Weight Polyethylene Reactor Powder," *Macromolecules*, 2002.
- [31] J. Chen, H. Zhao, Z. Xu, C. Zhang, J. Yang, C. Zheng and J. Lei, "Accelerated water tree aging of crosslinked polyethylene with different degrees of crosslinking," *Polymer Testing*, pp. 83-90, 15 September 2016.
- [32] S. Nilsson, T. Hjertberg and A. Smedberg, "Structural effects on thermal properties and morphology in XLPE," *European Polymer Journal*, pp. 1759-1769, 13 May 2010.
- [33] S. Nilsson, T. Hjertberg, A. Smedberg and V. Englund, "The Effect of Different Peroxide Decomposition Products on Selected Electrical Properties in XLPE," Gothenburg, 2010.
- [34] S. Mitra, A. Ghanbari-Siahkali, P. Kingshott, H. K. Rehmeier, H. Abildgaard and K. Almdal, "Chemical degradation of crosslinked ethylene-propylene-diene rubber in an acidic environment. Part II. Effect of peroxide crosslinking in the presence of a coagent," *Polymer Degradation and Stability*, vol. 91, pp. 81-93, June 2005.
- [35] G. M. Thomas, *The Rheology Handbook*, Vincentz Network, 2011.

SWEDISH SUMMARY

EN UNDERSÖKNING AV OLIKA TVÄRBINDNINGSSÄMNER FÖR HÖGSPÄNNINGSKABLAR MED AVSEENDE PÅ BIPRODUKTER SOM UPPSTÅR I PRODUKTEN UNDER PRODUKTIONEN

Inledning

För att kunna transportera el från en källa till en konsument behövs en kabel som kan transportera stora mängder el lätt och snabbt. För att kunna transportera stora mängder krävs det att materialen klarar av mycket höga spänningar (>500 kV), så kallad högspänd likström, HVDC. I dagens läge är det även viktigt att klara av långa sträckor av transport. Problem som uppstår är bland annat elförluster i samband med varje terminal som måste byggas var 50 km, då likström inte kan transporteras långa sträckor.

Kabeln är uppbyggd enligt följande, inifrån utåt: ledare, halvledande polyeten, tvärbunden polyetenisolation, ett andra lager halvledande polyeten, halvledande svällband med metallegering, stålmantel och polypropenmantel. De två halvledande polyetenlagren på var sin sida av isolationen extruderas på en gång, för att få en fullständig kontaktyta mellan alla lager. Uppsättningen beror på hur kabeln kommer att monteras eller var kabeln kommer att användas, dvs om det behövs extra skydd eller inte. Fokus i detta arbete ligger på de tre innersta lagren, dvs de två halvledande polyeten lagren och den tvärbundna polyetenisolationen. Den tvärbundna polyetenen tillför styrka och flexibilitet i kabeln. Isolationen bör klara av bland annat värme och extrema påfrestningar samt förebygga elektrisk urladdning. Det finns olika metoder och material som kan användas för att tillverka isolationen för att åstadkomma olika tvärbindningsgrader för att uppnå önskade egenskaper. Materialen och metoderna som används vid tillverkningen bör utvecklas, för att kablarna skall kunna transportera el längre sträckor och klara av högre kapaciteter. Detta ger grund för fortsatt forskning i ämnet.

Syfte

Syftet med forskningen var att jämföra olika föreningar som används för att tvärbinda polyeten, med utgångspunkt i olika patent för produktion av högspänningskablar med likström. Patent som använts tillhör Borealis, ABB och SILEC cable. Borealis och SILEC

cable tvärbinder med en peroxid, som är den vanligaste metoden för att tvärbinda på grund av peroxidens höga reaktionskänslighet. ABB använder sig av en azoförening, som jämfördes med en azoförening tillverkad vid Åbo Akademi. Azoföreningarna jämfördes även med peroxiderna. De fysikaliska egenskaperna, såsom tvärbindingstiden och tvärbindningsgraden, samt de bildade biprodukterna, analyserades och jämfördes med varandra.

Peroxider är väldigt reaktiva på grund av syret i molekylen ($-O-O-$). I tvärbindningsreaktionen bildas lätt alkoholer, som är polära molekyler. Polära molekyler försämrar ledningsförmågan, vilket rubbar eltransporten. Denna typ av oönskade produkter kallas biprodukter, och dessa bör undvikas i isolationen för en högspänningskabel. Laddningar samlar sig vid oregelbundenheter i materialets sammansättning som skapats av biprodukterna, vilket kan leda till elektrisk urladdning.

Azoföreningar har en typisk struktur med två kväveatomer, N, och en karbonylgrupp eller en bindning, X, som sedan fortsätter med ett kolväte, R, ($R'-X-N=N-X-R''$). Då azoföreningen reagerar frigörs N_2 -gas och CO_2 -gas som bildas av karbonylgruppen. Karbonylen kan även bli kvar i polymeren som en karbonyl tillsammans med kolvätesvansen.

Metod

Inledningsvis understrykes att Borealis blandning användes som referens och att den är riktgivande för vad som förväntas av en HVDC-kabelns egenskaper. Prover utfördes i ett laboratorium vid Åbo Akademi med recept tagna ur de patent för högspänningskablar som nämndes tidigare. Laboratorieproven var inte tvärbundna, utan enbart blandade tillsammans med värme till en homogen blandning. Proven användes till att mäta reologin där man får reda på hur materialets egenskaper förändras då massan smälter, proceseras och tvärbinds. Från testet fås tiden det tar för materialet att uppnå ”fullständig tvärbinding”. Dessa data var till nytta då proverna skulle köras i pilotmaskinen för att få fungerande processparametrar.

Fullskaliga prover gjordes i Maillefer Extrusion Oy:s pilotmaskin och proverna användes även för analys. Proverna från pilotmaskinen var kompletta prover som motsvarade verkliga produkter. Utifrån dessa prover analyserades tvärbindningsgraden med NMR och det utfördes en termisk analys av materialet med DSC. Utöver det utfördes även ett FTIR test för att bekräfta och se specifika bindningar som uppstår eller försvinner då olika tvärbindningsämnen används. De mekaniska egenskaperna mättes hos de tvärbundna proverna i form av hundben som utsätts för dragtest. Dessutom gjordes en extraktion av tvärbundet material. Detta för att få reda på den procentuella andelen tvärbundet material i proven, beräknat utifrån den vikt som förloras då otvärbundet material löser sig i lösningsmedlet.

Avslutningsvis utsattes rena ämnen som använts för tvärbindning av polymeren för ett pyrolystest med en pyrolys-GC/MS. På så sätt erhöles de biprodukter som kan uppstå då tvärbindningsämnena utsätts för höga temperaturer, som replikerar värmebehandlingen i slutskedet av kabelproduktionen för att sätta igång tvärbindningen.

Proverna skickades även till Tampereen Tekniillinen Yliopisto för mätning av resistivitet. Isolationen bör ha en så hög resistivitet som möjligt för att undvika problem under användningen. ”Borealis DC”-blandning innehållande peroxid som tvärbindningsmedel används som referens för god resistivitet.

Resultat och diskussion

Tillverkningen av laboratorieproverna gick väl, bortsett från att apparaturen som användes för blandningen var bristfällig i den mån att små mängder tillsatsämnen lätt fastnade på instrumentets väggar och att det var svårt att veta hur mycket tillsatsämnen som sist och slutligen hamnade i blandningen. Därför bör recepten nämnda i Appendix A – Recipes vara riktgivande.

Proverna som gjordes hos Maillefer Extrusion Oy var ”Borealis DC”, ”Borealis AC”, ”SILEC” och ”Åbo azo”. Recepten med Åbo Akademis azoförening jämförs med Borealis i olika test. Reologitesterna av de otvärbundna proverna bevisar att provet ”Åbo

azo” behövde en längre tid eller högre temperatur för att tvärbindas fullständigt jämfört med referensprovet. Vilket är en nackdel ur produktionssynvinkel.

Ur pyrolysis-GC/MS erhöles produkter som bildades då de olika receptens tvärbindningsämnen utsätts för höga temperaturer. Resultaten förväntades visa att azoföreningar inte bildar polära produkter då de sönderfaller, i motsats till peroxider. Produkter som bildades var i stort sett vad som förväntades, men resultaten verkade vara en aning avvikande eftersom azon visade sig innehålla till exempel polära ämnen. Detta kan dock ha berott på rester från ett tidigare prov. Det har bevisats teoretiskt, hur och varför ämnen som uppmätts uppstår, då Åbo Akademis azoföreningen sönderfaller. Från Figur 19 kan man konkludera att det inte bildats annat än opolära kolväten och kvävgas.

Tvärbindningsgraden undersöks med DSC, NMR, och med ett gel test. Med NMR mäts protonernas (^1H) eko som utgör relaxionen i polymerens struktur. Resultatet fås som intensiteten i förhållande till tiden. Högre tvärbindning ger en styvare struktur, vilket försnabbar relaxionen av polymeren. Resultaten visar att ”Borealis DC” har den styvaste strukturen, följt av ”Borealis AC”, ”SILEC” och sist ”Åbo azo”. Resultaten står en aning i konflikt med teorin, eftersom det är känt att ”Borealis DC” har en lägre peroxidhalt än ”Borealis AC” och ”SILEC”, då dessa i teorin borde ha en aningen styvare struktur än ”Borealis DC”. DSC förväntas visa en lägre kristallinitet hos ämnen med tätare tvärbunden struktur, då molekylerna i materialet inte kan bilda kristaller på grund av tvärbindningen. DSC resultaten påvisar högsta kristalliniteten för ”Åbo azo”, följt av ”SILEC”, ”Borealis AC” och sist ”Borealis DC”. Andelen gel fås genom att koka proven i p-xylene i 24 timmar. Med andelen gel menas andelen tvärbundet material som bildats. Tätare tvärbindning ger en högre andel gel. Resultaten påvisade att ”Borealis DC” innehåller 69 % gel, ”Borealis AC” 87 %, ”SILEC” 84 % och ”Åbo azo” 80 %. Resultaten var inte förväntade eftersom ”Borealis DC” borde ha haft den högsta tvärbindningsgraden, ca 80%. Även noll-provet som borde upplösas helt i p-xylenet, upplöstes endast delvis, vilket är ett tecken på att testet var opålitligt.

FTIR ger information om bindningar i molekyler. FTIR-spektrumet på de tvärbundna proven visar för ”Borealis DC” en kurva likt ett rent LDPE material. De andra proven

visar varsin signaltopp på områden för aldehyder, (C=O). För "SILEC" och "Borealis AC" visar sig spektrummen inte innehålla övriga bindningar eller funktionella grupper. "Borealis AC" har en aning mer signaler än "SILEC" men inga märkvärdiga. "Åbo azo" har en hel del signaltoppar mellan 1400 och 800 cm^{-1} . Området 900–700 cm^{-1} är typiskt för olika C-H töjningar o vibrationer, vilket inte är ett problem med tanke på att polära ämnen bör undvikas. I spektrumet hittas även en signaltopp som kan komma från en etergrupp, en aminstretch eller både och. Eter-gruppen skulle ha en negativ inverkan på ledningsförmågan. En annan relativt hög signaltopp observeras också, som troligen är en dubbelbindning C=C eller amingrupp. De polära ämnen som observerats i "Åbo azo"-provet kommer troligtvis av en tvärbindnings-hjälp molekyl (TAC) som användes i tillverkningen av provet för att höja tvärbindningens täthet. TAC-molekylen innehåller syreatomer, vilket kunde vara orsaken till att polära ämnen bildats.

Mekaniska egenskaper mättes med dragtest i rumstemperatur och i 95 °C. I rumstemperatur var resultaten mycket lika, "Åbo azo"-provet hade en aning lägre styrka jämfört med de andra proven, 24 MPa jämfört med 30 MPa för andra. Då temperaturen höjs ökar töjningen hos "Borealis DC" och "Åbo azo" medan töjningen förblir mindre för "SILEC" och "Borealis AC" jämfört med proven i rumstemperatur. "Borealis DC" har den högsta dragstyrkan på 10.4 MPa vid den förhöjda temperaturen och följt av "Åbo azo" med 7,5 MPa.

Resistiviteten mättes i "Borealis DC", "SILEC" och "Åbo azo" proven från pilotmaskinen. Resultaten påvisar att "Borealis DC" och "SILEC" är så gott som lika, båda har en magnitud på 10^{14} . "Åbo azo" förblir en magnitud lägre, 10^{13} , då styrkan på det elektriska fältet är 10 kV/mm. Proven utsätts även för högre styrka och med ökad styrka försämrades resistiviteten i "Åbo azo"-provet ytterligare några magnituder.

Slutligen kan påpekas att det var möjligt med den nya azoföreningen från Åbo Akademi, att i pilotmaskinen tillverka en kabel som motsvarar de kablar som finns på marknaden. Azo-föreningarna kräver en högre temperatur och dessutom bör mera tvärbindningsämnen tillsättas i polymeren för att uppnå samma eller liknande resultat som

Jessica Malmberg

kablar på marknaden. Fortsatt forskning borde fokusera på att optimera doseringen för azoföreningar och att hitta rätt tvärbindningshjälpmedel för förbättrad tvärbindning.

APPENDICES

Appendix A – Recipes

Recipe for testing of by-products and rheological measurements.

Recipe 1. SILEC	Compound	Amount (%)	Amount (g)	Actual (g)	True %
1.1	Ineos BPD-2000	100 %	35	35,0275	
	Crosslinking agents	1,35 %	0,4725	0,490	1,3986 %
	TAICROS	70 %	0,33075	0,3347	68,32 %
	Trigonox 101	30 %	0,14175	0,1552	31,6799 %
	Antioxidants	0,08 %	0,028	0,033	0,0951 %
	Irganox 1076	50 %	0,014	0,0173	51,9520 %
	Irganox PS8000	50 %	0,014	0,016	48,0480 %

1.2	Compound	Amount (%)	Amount (g)	Actual (g)	True %
	Ineos BPD-2000	98,58 %	34,503	35,3411	98,4997 %
	Crosslinking agents	1,150 %	0,403	0,442	1,251 %
	TAICROS	0,8 %	0,280	0,293	0,8285 %
	Trigonox 101	0,35 %	0,1225	0,1492	0,4222 %
	Antioxidants	0,27 %	0,0945	0,0963	0,2725 %
	Irganox 1076	50 %	0,04725	0,0476	49,4289 %
	Irganox PS8000	50 %	0,04725	0,0487	50,5711 %

Recipe 2. ABB	Compound	Amount (%)	Amount (g)	Actual (g)	true%
2.1	Ineos BPD-2000	100 %	35	35,1045	
	Crosslinking agents	1,35 %	0,4725	0,51	1,4622 %
	DBAC	50 %	0,23625	0,2459	47,9057 %
	TAC	50 %	0,23625	0,2674	52,0943 %
	Antioxidants	0,08 %	0,028	0,0297	0,0846 %
	Irganox 1076	50 %	0,014	0,0154	51,8519 %
	Irganox PS8000	50 %	0,014	0,0143	48,1481 %

2.2	Compound	Amount (%)	Amount (g)	Actual (g)	True %
	Ineos BPD-2000	100 %	35	35,3285	
	Crosslinking agents	4 %	1,400	1,408	4 %
	DBAC	2 %	0,700	0,704	1,9922 %
	TAC	2 %	0,700	0,704	1,9919 %
	Antioxidants	0,035 %	0,01225	0,0130	0,0368 %
	Irganox 1076	0,01 %	0,0035	0,0039	0,0110 %
	Irganox PS8000	0,025 %	0,00875	0,0091	0,0258 %

No antioxidants mentioned in patent, based on recommendations found on po

Recipe 3. Åbo Azo Compound		Amount (%)	Amount (g)	Actual (g)	true%
3.1	Ineos BPD-2000	100 %	35	35,0463	
	Crosslinking agents	1,35 %	0,4725	0,5346	1,5254 %
	Azo-compound	50 %	0,23625	0,2429	45,4358 %
	TAC	50 %	0,23625	0,2917	54,5642 %
	Antioxidants	0,08 %	0,028	0,029	0,0827 %
	Irganox 1076	50 %	0,014	0,0144	49,6552 %
	Irganox PS8000	50 %	0,014	0,0146	50,3448 %

3.2	Compound	Amount (%)	Amount (g)	Actual (g)	True %
	Ineos BPD-2000	100 %	35	34,996	
	Crosslinking agents	4 %	1,400	1,4207	4,0596 %
	Azo-compound	2 %	0,700	0,7207	2,0594 %
	TAC	2 %	0,700	0,7	2,0002 %
	Antioxidants	0,035 %	0,01225	0,0127	0,0363 %
	Irganox 1076	0,01 %	0,0035	0,0044	0,0126 %
	Irganox PS8000	0,025 %	0,00875	0,0083	0,0237 %

Appendix B – Process parameter data from pilot machine

